Clinical Immunology 248 (2023) 109251

Contents lists available at ScienceDirect

Clinical Immunology

journal homepage: www.elsevier.com/locate/yclim

Ectopic lymphoid structures in the aged lacrimal glands

Jeremias G. Galletti [a,b], Kaitlin K. Scholand [a,c], Claudia M. Trujillo-Vargas [a,d], Zhiyuan Yu [a], Olivier Mauduit [e], Vanessa Delcroix [e], Helen P. Makarenkova [e], Cintia S. de Paiva [a,*]

[a] Ocular Surface Center, Department of Ophthalmology, Cullen Eye Institute, Baylor College of Medicine, Houston, TX, USA
[b] Institute of Experimental Medicine (CONICET), National Academy of Medicine of Buenos Aires, Buenos Aires, Argentina
[c] Biochemistry and Cell Biology Graduate Program, Department of BioSciences, Rice University, Houston, TX, USA
[d] Grupo de Inmunodeficiencias Primarias, Facultad de Medicina, Universidad de Antioquia, UdeA, Medellín, Colombia
[e] Department of Molecular Medicine, The Scripps Research Institute, 10550 North Torrey Pines Road, La Jolla, CA 92037, USA

ARTICLE INFO

Keywords:
Aging
Ectopic lymphoid structures
Tertiary lymphoid organs
Lacrimal gland
Dry eye
B cells

ABSTRACT

Aging is a complex biological process in which many organs are pathologically affected. We previously reported that aged C57BL/6J had increased lacrimal gland (LG) lymphoid infiltrates that suggest ectopic lymphoid structures. However, these ectopic lymphoid structures have not been fully investigated. Using C57BL/6J mice of different ages, we analyzed the transcriptome of aged murine LGs and characterized the B and T cell populations. Age-related changes in the LG include increased differentially expressed genes associated with B and T cell activation, germinal center formation, and infiltration by marginal zone-like B cells. We also identified an age-related increase in $B1^+$ cells and $CD19^+B220^+$ cells. $B220^+CD19^+$ cells were $GL7^+$ (germinal center-like) and marginal zone-like and progressively increased with age. There was an upregulation of transcripts related to T follicular helper cells, and the number of these cells also increased as mice aged. Compared to a mouse model of Sjögren syndrome, aged LGs have similar transcriptome responses but also unique ones. And lastly, the ectopic lymphoid structures in aged LGs are not exclusive to a specific mouse background as aged diverse outbred mice also have immune infiltration. Altogether, this study identifies a profound change in the immune landscape of aged LGs where B cells become predominant. Further studies are necessary to investigate the specific function of these B cells during the aged LGs.

1. Introduction

As we age, all our organs are subjected to progressive changes that finally lead to dysfunction and death. However, in some individuals these changes are accompanied by exacerbated inflammation which translates into symptoms such as discomfort, pain and a decrease in the quality of life. In the eye, advanced age is a risk factor for dry eye disease (also named sicca syndrome), a dysfunction in the lubrication capabilities of the ocular surface characterized by symptoms of irritation and inflammatory damage [1]. One of the most important components of the ocular surface is the lacrimal gland, which secretes the aqueous component of the tear film. As part of the mucosal immune system, the lacrimal glands are constantly surveilled by immune cells that collaborate in the clearance of foreign antigens captured through the ocular surface and irrigating blood vessels [2,3]. Remarkably, the recruitment and residency of these cells increases with age and is directly associated with the pathological changes in lacrimal gland physiology marked by inadequate lubrication and immunity [4–12].

Murine and human lacrimal glands have increased lymphocytic infiltration as they age [4–12]. In many instances, the recruitment of immune cells with aging mirrors an immune invasion and triggers the formation of lymphoid structures with certain degree of T and B cell segregation and the presence of follicular dendritic cells and high endothelial venules. These structures stimulate antigen capture and presentation with the subsequent growth and differentiation of clonal expansion-derived lymphocytes. Often referred to as ectopic lymphoid structures or tertiary lymphoid tissue, these cell aggregates frequently lack the immune checkpoints of secondary lymphoid organs and therefore represent the niche of auto-antibody production against locally-expressed antigens [13]. Interestingly, ectopic lymphoid

* Corresponding author at: Cullen Eye Institute, Department of Ophthalmology, Baylor College of Medicine, 6565 Fannin Street, NC 505G, Houston, TX 77030, USA.
E-mail addresses: Kaitlin.Scholand@bcm.edu (K.K. Scholand), claudia.trujillo@udea.edu.co (C.M. Trujillo-Vargas), zhiyuan.yu@bcm.edu (Z. Yu), omauduit@scripps.edu (O. Mauduit), vdelcroix@scripps.edu (V. Delcroix), hmakarenk@scripps.edu (H.P. Makarenkova), cintiadp@bcm.edu (C.S. de Paiva).

https://doi.org/10.1016/j.clim.2023.109251
Received 1 December 2022; Received in revised form 22 January 2023; Accepted 24 January 2023
Available online 3 February 2023

structures are formed independently of key factors needed for the development of secondary lymphoid organs such as lymphotoxin upon the expression of inflammatory cytokines. Ligon and colleagues performed a detailed mapping of ectopic lymphoid structures in the bladder of aged mice, reporting the presence of naïve, activated and germinal center B cells and IgA^+ plasma cells, a process independent of the microbiota but dependent on TNF-α [14].

Another interesting area of investigation are the factors that predispose the body to exhibit exacerbated inflammation in certain organs. Our group has mainly worked with animal models and among them, we have used the C57BL/6J (B6) strain of mice because it is widely used in the aging field. Furthermore, these mice develop predominantly a Th1/Th17 immune response, which corresponds to the immune response in human dry eye patients [15–17]. However, distinctive vitamin A metabolism and therefore mucosal immunity, have been observed in B6 mice, which make them more prone to develop exacerbated inflammation in the surfaces [18]. Moreover, although genetic homogeneity of inbred strains facilitates experimental replicability, this may also oversimplify and bias biological phenotypes in outbred populations such as humans [18]. Therefore, outbred mice models have been investigated in several models of diseases and some characteristics seen in inbred null mice were maintained in the outbred mice. An example is the generation of Fam83h knockout mice by CRISPR/Cas9-mediated gene engineering that showed delayed eye opening and dry eye [19].

In this study, we analyzed the transcriptome of aged murine lacrimal glands, characterized the B cell populations among the immune infiltrates and compared them with that of lacrimal glands from a Sjögren syndrome mouse model. Also, we investigate ectopic lymphoid structures formation in lacrimal glands from an outbred strain of mice. Our data confirmed increased presence of ectopic lymphoid structures in the aged-inbred mouse lacrimal gland. The topmost upregulated genes in the aged gland are involved in B cell- followed by T cell-activation and T:B cell help. We also observed a progressive increase in the expression of germinal center markers with age and the presence of IgM and IgG1 in the gland, which suggest isotype switching *in situ*. These findings are similar to the ones observed in the lacrimal gland from young mice from a mouse model of Sjögren syndrome. Our data also demonstrated that ectopic lymphoid structures formation and altered ocular surface lubrication are also present in the aged lacrimal gland from outbred female mice. Despite this finding, a decreased frequency of goblet cells in the conjunctiva was observed in female as well as male outbred mice.

2. Material and methods

2.1. Animals

The Institutional Animal Care and Use Committee at Baylor College of Medicine, The Scripps Research Institute and Jackson Laboratories approved all animal experiments. In addition, all studies adhered to the Association for Research in Vision and Ophthalmology for the Use of Animals in Ophthalmic and Vision Research and the NIH Guide for the Care and Use of Laboratory Animals [20]. The experiments were performed at the Ocular Surface Center, Department of Ophthalmology, Baylor College of Medicine (Houston, TX), the Scripps Research Institute (La Jolla, CA) and at the Jackson Laboratories (Bar Harbor, ME).

B6 animals were purchased from the Jackson Laboratories (Bar Harbor, ME), aged in-house, or received from the National Institute of Aging. They were used at 2–3 months (young, $n = 31$); 12–14 months (middle-aged, $n = 48$), 16 months ($n = 8$), and 22–26 months (aged, $n = 37$). Tissues (lacrimal glands and eyes with eyelids) from *diversity outbred mice* (DO, IMSR_JAX:009376, Jackson Laboratories, Bar Harbor, ME) were collected at Jackson Laboratories and shipped to Baylor College of Medicine. There were 20 young (8–12 weeks, $n = 10$ females, 10 males) and 20 aged mice (24 months, 10 males, 10 females).

Mice were housed in specific pathogen-free facilities of Baylor College of Medicine, The Scripps Research Institute and Jackson Laboratories and were kept on diurnal cycles of 12 h/light and 12 h/dark with *ad libitum* access to food and water and environmental enrichment. Because dry eye is more frequent in women [21,22], and aged male mice do not develop corneal barrier disruption (a hallmark of dry eye) [23], the majority of the study used B6 female mice, unless otherwise noted. An effort was made to collect multiple tissues from each mouse. Tear volume and tears washings were collected from live animals. A final sample size per endpoint can be found in figure legends.

2.2. Measurement of tear volume

Clement Clarke Schirmer Tear Test strips (Veatch Ophthalmic Instruments, Tempe, AZ) were cut in half longitudinally to yield strips that measured 2 mm wide x 40 mm long. Tear measurements were performed in live animals; strips were placed in the inferior eyelid and allowed to wet for 30 s. The length of stripping was then measured with a scientific ruler.

3. Tear washings and multiplex cytokine immunobead assay

Tear washings were collected from young (2 M) and 16 M female B6 mice. Briefly, 1.5 μl of phosphate-buffered saline containing 0.1% bovine serum albumin was instilled into the conjunctival sac. The tear fluid and buffer were collected with a 1 μl volume glass capillary tube (Drummond Scientific Co, Broomhall, PA) by capillary action from the tear meniscus in the lateral canthus and stored at 80 °C until the assay was performed. One sample consisted of tear washings from both eyes of two mice pooled (4 μl) in phosphate-buffered saline with 0.1% bovine serum albumin (6 μl). There were 5 to 10 samples per group: one sample equals tear washing pooled from 4 eyes. Samples were added to wells containing the appropriate cytokine bead mixture that included mouse monoclonal antibodies specific for TNF-α, chemokine CXC motif ligand 1 (CXCL1) ligand 1, and VEGF (Millipore, Burlington, MA), as previously reported [24]. The reactions were detected with streptavidin-phycoerythrin using a Luminex 100 IS 2.3 system (Austin, TX). Results are presented as mean ± SD (pg/ml). The inferior levels of detection were 2.9 pgm/ml (TNF-α), 1.5 pg/ml (VEGF), and 1.92 (CXCL1) pg/ml.

4. RNA isolation and Real-time PCR

4.1. Extraorbital lacrimal glands were excised and the whole glands were lysed in RNA lysis buffer

Total RNA from lacrimal glands was extracted using a QIAGEN RNeasy Plus Mini RNA isolation kit (Qiagen; Hilden, Germany) following the manufacturer's protocol. After isolation, RNA concentration was measured, and cDNA was synthesized using the Ready-To-Go You-Prime First-Strand kit (GE Healthcare, Chicago, IL).

Real-time PCR was performed using specific TaqMan minor groove binder probes for CD19 (*Cd19,* Mm00515420), CXCL13 (*Cxcl13*, Mm00444533), Glycam-1 (*Glycam1*, Mm00801716_m1), CXCR5 (*Cxcr5*, Mm00432086), CCR7 (Ccr7, Mm00432608) CD22 (*Cd22*, Mm00515432), IL-21 (*Il21*, Mm00517640), CXCL12, (*Cxcl12*, Mm00445553), LTB (*Ltb*, Mm00434774), CCL19 (Ccl19, Mm00839967), BAFF (*Tnfsf13b*, Mm00446345) and TaqMan Universal PCR Master Mix AmpErase UNG in a commercial thermocycling system (StepOnePlus Real-Time PCR System Applied Biosystems/Thermo Fisher Scientific, Foster City, CA), according to the manufacturer's recommendations. The hypoxanthine phosphoribosyltransferase 1 (*Hprt1*; Mm00446968) gene was used as an endogenous reference for each reaction. The quantitative PCR results were analyzed by the comparative Ct method and were normalized by the Ct value of Hprt1. The young group served as calibrators.

4.2. Histology, PAS Staining, IHC, and quantification of focus score

Eyes and ocular adnexa were excised, fixed in 10% formalin, paraffin-embedded, and cut into 5-μm sections using a microtome (Microm HM 340E, Thermo Fisher Scientific Waltham, MA). Sections cut from paraffin-embedded globes were stained with Periodic Acid Schiff (PAS) reagent. The goblet cell density was measured in the superior and inferior bulbar and tarsal conjunctiva using NIS-Elements software (AR, version 5.20.2; Nikon Melville, NY) and expressed as the number of positive cells per millimeter. [25].

Immunofluorescence was performed to detect CD3 (catalog# MCA1477A647, AlexaFluor®647, clone CD3–12; BIO-RAD, Hercules, California), B220 (AlexaFluor®488-B220, clone RA3-6B2; BIO-RAD, MCA1258A488); IgM (catalog 115–585-020, Alexa Fluor® 594 AffiniPure Goat Anti-Mouse IgM, Jackson ImmuneResearch, West Grove, PA) PNAd (catalog #553863, clone MECA-79, BD Biosciences, Franklin Lakes, New Jersey), goat-anti-mouse LYVE-1 (sc-19,319, Santa Cruz Biotechnologies, Santa Cruz, CA) antibodies using cold acetone fixation and 20% BSA serum as blocking solution. Secondary goat anti-rabbit Alexa-Fluor® 488 or 594 conjugated IgG antibodies were used, as previously described [26]. The images were captured and photographed by an Eclipse E400 Nikon fluorescence microscope equipped with a DS–F1 digital camera.

Lymphocytic infiltration foci were counted in hematoxylin and eosin-stained lacrimal gland sections by standard light microscopy using a 10× objective (Nikon, Eclipse E400) by two masked observers. A minimum of 50 mononuclear cells was counted as one focus, and the total number of foci per gland was recorded. Slides were scanned to obtain digital images using PathScan Enabler V (Meyer Instruments, Houston, TX) and were calibrated according to the manufacturer's instructions (2.54um/px) using NIS Elements software. The lacrimal glands' total area was measured using the "autodetect area" function of the Nikon Elements software or was manually circumscribed using the polyline function. Finally, focus scores were calculated by dividing the number of foci per mm^2 and quantifying the number of inflammatory cell foci per 4 mm^2 tissue area.

4.3. Flow cytometry analysis

As previously reported, single-cell suspensions of the lacrimal glands, conjunctival, and cervical lymph nodes were prepared [24]. 1×10^6 cells from the single-cell suspensions of the lacrimal gland and cervical lymph nodes ($n = 7$ to 10/ group) were plated and then stained with different panels. Cells were blocked with CD16/CD32, washed, incubated with live/dead cell discriminator (IR, Invitrogen-Molecular Probes), and then stained using different panels as below.

For germinal center evaluation, cells were stained with CD45 (BV510, clone 30F11, Biolegend, catalog#103138), B220 (clone RA3-6B2, BD Biosciences, catalog#553092), GL7 (PERCP CY5.5, Biolegend, Catalog#144610), CD95 (Anti-CD95 PE, Biolegend Catalog#152608). The following gating strategy was used: live $CD45^+$ cells were gated by excluding live/dead cells, followed by two sequential single-cell gates. $B220^+$ cells were plotted again vs. side scatter area and further gated into $GL7^+$ and $CD95^+$ cells. The presence of autofluorescence (attributed to an age-related increase in lipofuscin) [27] is more evident in some wavelengths than others. To circumvent this, we gated $CD95^+GL7^+$ cells based on fluorescence minus control from lacrimal gland cell suspensions.

To investigate the frequency of T follicular helper cells, we used the following antibodies: anti-CD45 (BV510, clone 30F11, Biolegend), CD4 (FITC, clone RM4–5, Invitrogen/ThermoFisher, catalog #11–0042-86), CXCR5 (PE, clone L138D7 Biolegend, catalog #145504), PD-1 (BV421, clone 29F.1A12, Biolegend, catalog #135218), BCL-6 (PE_CY7, clone 7D1, Biolegend, catalog#358512), and IL-21 (APC, clone FFA21, ThermoFisher, catalog#17–7211-82). For this panel, single-cell suspensions were incubated with PMA and ionomycin for 5 h [11]. The following gating strategy was used: live $CD45^+$ cells were gated by the exclusion of live/dead dye, followed by two sequential single-cell gates. $CD4^+$ T cells were plotted and identified. Among $CD4^+$ T cells, CXCR5 was plotted versus PD-1 and $CXCR5^+PD\text{-}1^+$ cells were further examined based on the expression of BCL-6 and IL-21.

To examine the frequency of marginal zone B cell, B follicular, and transitional cells, the following panel was used. anti-CD45 (BV510, clone 30F11), B220 (clone RA3-6B2), CD93 (PECY7, clone AA41, Biolegend, Catalog#136506), IgM (FITC, clone RMM-1, Biolegend, Catalog#406506) CD23 (BV421, clone B3B4, Biolegend, catalog#101621). Cells were washed and then kept on ice until data acquisition. The following gating strategy was used: live $CD45^+$ cells were gated by the exclusion of live/dead dye, followed by two sequential single-cell gates. $B220^+$ cells were plotted again vs. side scatter area and further gated into $CD93^+$ and $CD93^-$ cells. Cell populations were then plotted as IgM vs. CD23 and gates were made based on fluorescence minus one control.

A separate experiment verified the frequency of CD19 and B220 by using the following antibodies: CD45 and B220 (as above) and CD19 (APC, clone 6D5, BioLegend, catalog #115512).

A BD LSRII Benchtop cytometer was used for data acquisition and data was analyzed using BD Diva Software (BD Pharmingen) and FlowJo software (version 10.1; Tree Star, Inc., Ashland, OR, USA). Biological replicates were averaged.

4.4. Multiplex bead array for BAFF and CCL21

Lacrimal glands from B6 mice of different ages ($n = 10$/age) were harvested and lysed in cell lysis buffer 2 (R&D Systems, Minneapolis, MN, Cat# 895347). Protein concentration was measured using a micro-BCA protein assay kit (Thermo Fisher, Waltham, MA, Cat# 23235). Sample reactions were set up according to the manufacturer protocol from the kit (R&D Systems, Minneapolis, MN). Lacrimal gland extracts (100 μg) were resuspended in calibrator diluent and a diluted microparticle cocktail was added for 2 h at room temperature. After washing, a diluted biotin-antibody cocktail was added and incubated for 1 h at room temperature. Washed samples again and then diluted streptavidin-PE added and incubated for 30 min at room temperature. Finally, samples were read using a Luminex Instrument (xPONENT 3.1, Luminex 100 IS Version 2.3, Austin, TX). Cytokines and chemokines (BAFF, CCL21) concentration were measured by software (Millipex analyst version 5.1, Millipore, Burlington, MA). The minimum detectable level is 64.7 pg/ml for BAFF and 2.5 pg/ml for CCL21.

4.5. Bulk RNA sequencing and data analysis

The whole extraorbital lacrimal glands were excised from B6 female mice at 2 months-old (M), 12 M and 24 M in triplicates and lysed into a tube containing RNA lysis buffer (Qiagen, Valencia, CA, USA).Total RNA was extracted using a QIAGEN RNeasy Plus Micro RNA isolation kit according to the manufacturer's instructions. The concentration and purity of RNA were assessed using a NanoDrop 1000 (ThermoFisher Scientific, Waltham, MA, USA). RNA-Seq was performed by the Beijing Genomics Institute (BGI) using the BGISEQ500RS to generate 100 bp paired-end reads. The raw data were cleaned by removing reads containing adapter or poly-N sequences, and reads of low quality using SOAPnuke (v. 1.5.2, parameters: –l 15 – q 0.2 – n 0.05), and the expression levels of the resulting genes and transcripts were determined using RSEM (v. 2.2.5, default parameters). Data was analyzed by ROSALIND® (https://rosalind.bio/), with a HyperScale architecture developed by ROSALIND, Inc. (San Diego, CA). Reads were trimmed using cutadapt [28]. Quality scores were assessed using FastQC. Reads were aligned to the *Mus musculus* genome build GRCm38 using STAR [29]. Individual sample reads were quantified using HTseq [30] and normalized via Relative Log Expression (RLE) using DESeq2 R library [31]. Read Distribution percentages, violin plots, identity heatmaps, and sample MDS plots were generated as part of the QC step using RSeQC

[32]. DEseq2 was also used to calculate fold changes and *p*-values and perform optional covariate correction. Clustering of genes for the final heatmap of differentially expressed genes was done using the PAM (Partitioning Around Medoids) method using the fpc R library. Hypergeometric distribution was used to analyze the enrichment of pathways, gene ontology, domain structure, and other ontologies. The topGO R library [33], was used to determine local similarities and dependencies between GO terms in order to perform Elim pruning correction. Several database sources were referenced for enrichment analysis, including Interpro [34], NCBI [35], MSigDB [36] REACTOME [37], WikiPathways [38]. Enrichment was calculated relative to a set of background genes relevant for the experiment.

4.6. Biological pathway analysis

From the list of differentially expressed genes (DEGs) identified by RNAseq, we used Gene Ontology database (http://geneontology.org/) to identify the altered biological pathways. To achieve this, we submitted the lists of DEGs and performed a GO enrichment analysis. Then, we selected only the top-10 of biological pathways based on fold enrichment and the FDR < 0.05. Heatmaps of significantly altered pathways were generated using GraphPad Prism (GraphPad Software, San Diego, CA, version 9.2).

4.7. Detection of anti-Ro52/SSA and anti-La/SSB autoantibodies

Blood was collected through cardiac puncture after euthanasia and serum was isolated after centrifugation from female B6 mice of different ages. Mouse anti-Ro52/SSA and anti-La/SSB ELISAs (Catalog EA5203 and EA5204, respectively, Signosis Inc., Santa Clara, California) were used according to the manufacturer's protocol. Serum samples from mice were diluted at 1:50 and a standard curve was applied. Serum samples from male NOD·B10.H2^b mice that had been archived and stored at -80°C were used a positive control.

4.8. Comparison between Sjögren syndrome and aging

To decipher the shared and specific molecular alteration between aging and autoimmune disease, we compared the expression patterns of the genes altered in aging animals and the mouse strain NOD·B10.H2^b, a model for Sjögren syndrome. In this mouse strain, lacrimal gland inflammation is more prevalent inmales than in females [39]. At the age 4 months (4 M), NOD.B10.H2^b male mice fully develop lacrimal gland inflammation but are free from age-related effects. Therefore, respective DEGs of each RNA-seq dataset were obtained by comparing 24 M to 2 M female B6 (aging), and 4 M males NOD.B10.H2^b to BALB/c [39] using a threshold of fold change <-1.5 or > 1.5 and a *p*-value adjusted <0.05. With Rosalind's web-based software, we performed a meta-analysis using a machine-based clustering algorithm to group each gene set depending on their expression pattern. Each list of genes given by the different patterns has been submitted into www.metascape.org with default parameters to obtain the pathways significantly enriched according to different databases. The top 3 of most significant pathways -Log10(*P*-value) for each pattern have been plotted and colorized depending on their enrichment p-value.

4.9. Statistical analysis

Based on pilot studies, the sample size was calculated with StatMate2 Software (GraphPad Software, San Diego, CA). Statistical analyses were performed with Graph Pad Prism software (GraphPad Software, San Diego, CA, version 9.2). Data were first evaluated for normality with the Kolmogorov-Smirnov normality test. Appropriate parametric (*t*-test) or non-parametric (Mann-Whitney) statistical tests were used to make comparisons between the two age groups. Whenever adequate, one-way or two-way ANOVA or Kruskal-Wallis followed by post hoc tests were used. All experiments were repeated at least once. The final sample per experiment is shown in the figure legends.

5. Results

5.1. Increased B and T cell infiltration in aged lacrimal glands

Aging is a risk factor for dry eye, a multifactorial disease characterized by a dysfunctional tear film [22,40–42]. We and others reported that aged mice develop cardinal signs of dry eye, including corneal staining (increased corneal permeability), loss of corneal nerves and corneal surface regularity, conjunctival goblet cell loss, and signs of Meibomian gland disease [23,43–50]. Tear volume measured at the inferior meniscus of the eyelid is the sum of tear fluid and conjunctival fluid, and there is increased conjunctival permeability in inflamed tissues, such as the aged conjunctiva [51,52]. Dry eye is characterized by a dysfunctional tear filminf quantity, quality, or both [42]. We previously showed that despite having increased tear volume [43], aged mice exhibit increased concentration levels of certain inflammatory cytokines and significantly lower VEGF concentration levels [24]. Some of these inflammatory markers are responsive to anti-inflammatory therapy [53]. However, aged mice are also larger and when tear volume was normalized by body mass, the ratio between tear volume and body mass stayed constant as mice aged [54]. In this study, we confirmed our previous findings that female B6 mice have increased tear volume as they age (Fig. 1A). Using multiplex Luminex analysis, we confirmed decreased levels of VEGF but increased tears levels of TNF-α, and CXCL1 (Fig. 1B). Thus, the tear film in aged mice is dysfunctional in quality and contributes to a dysregulated ocular surface environment. Considering this, we then examined the aged extraorbital lacrimal glands as they are responsible for the secretion of the aqueous part of the tear film.

Several organs exhibit ectopic lymphoid structures formation with aging [14,55]. In the murine liver, these structures are associated with the presence of inflammatory mediators and immunoglobulin and recombinase gene transcripts [56]. We and others previously reported that murine lacrimal glands develop immune infiltrates with aging and chronic inflammation [43,57]. The infiltrating immune cells are easily identified adjacent to ducts and forming lymphocytic foci [24,58]. We quantified immune infiltration in H&E histological sections and noted that, although variable, the increase in these inflammatory foci is detected as early as 12months of age in B6 mice (Fig. 1C-D), in agreement with our previous publications [24]. We stained aged lacrimal glands and observed that the infiltrates are loosely organized into T and B zones (Fig. 1E). The majority of the infiltrates are B cells (Fig. 1F) although CD3$^+$ T cells are also present [57]. Flow cytometry validated the immunostaining findings, which confirmed a higher proportion of CD19$^+$B220$^+$ B cells among CD45$^+$ cells. Interestingly, B1B cells (CD19$^+$B220$^-$) also increased with aging, while CD19$^-$B220$^+$ decreased (Fig. 1G-H). qPCR in lacrimal gland lysates confirmed increased expression of *Cd19* and *Cd22* transcripts (Fig. 1I).

5.2. Transcriptome analysis of aged lacrimal glands shows B and T cell activation as top upregulated pathways

Next, we investigated the impact of B and T immune infiltrates by performing bulk RNA sequencing of the extraorbital lacrimal glands of young (2 M) and aged (24 M) female B6 mice. In this analysis, 2220 DEGs with a fold change of at least 1.2 and a false discovery rate (FDR) $<$ than 0.05 were identified; of these, 1317 DEG were upregulated while 903 were downregulated (Fig. 2A, Supplemental Table 1). A volcano plot graphically shows the gene distribution (Fig. 2B). Regarding the impact of immune infiltrates in the aged lacrimal gland, several of the topmost upregulated genes were related to B cell activation and homeostasis: *Ighm* (encoding the constant region of the heavy IgM chain), *Pou2af1* (a B-cell transcription factor) [59], *Cd79a* (alpha chain of B-cell antigen receptor complex-associated protein), *Cxcl13* (a B cell

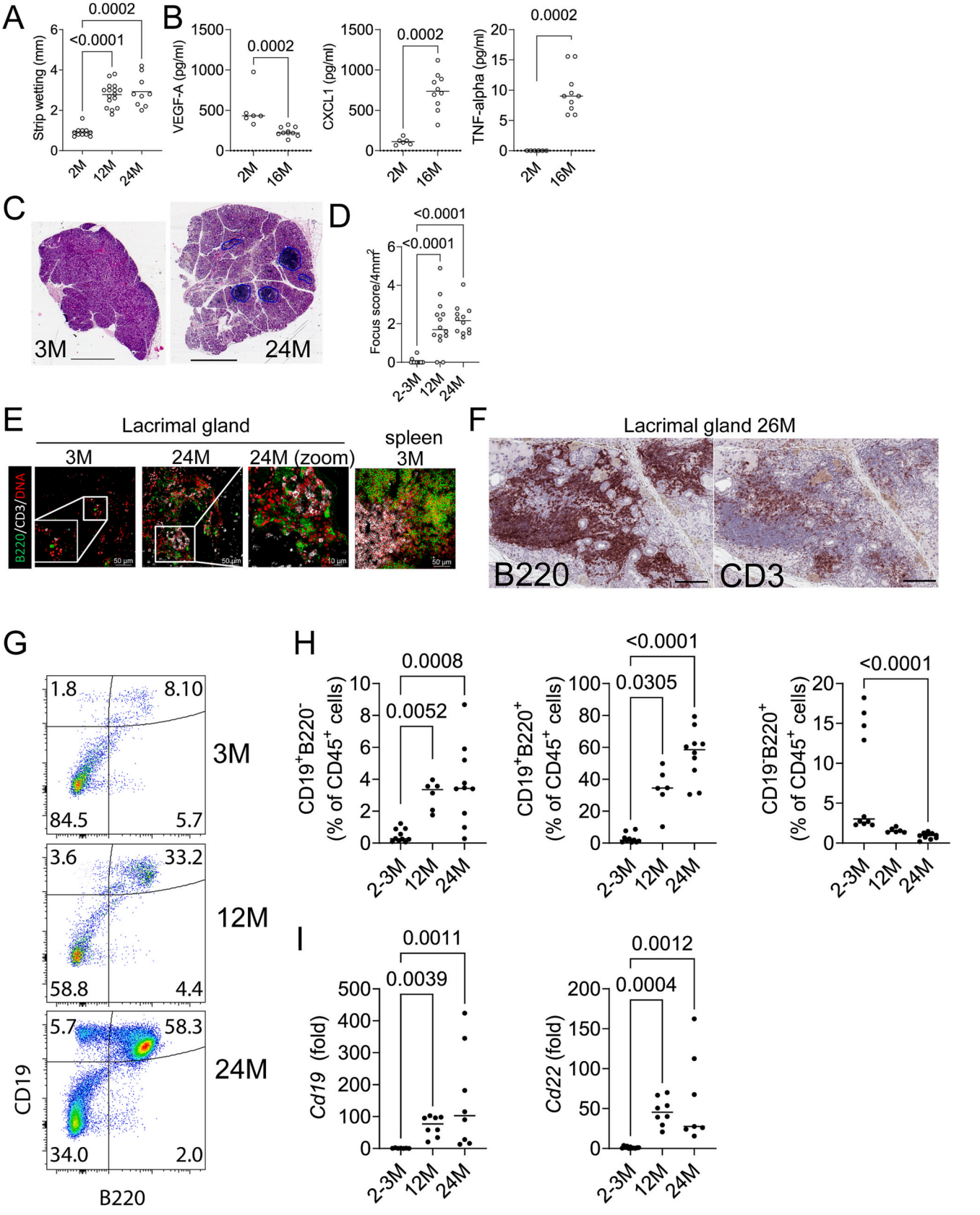

(caption on next page)

Fig. 1. Increased B cell infiltration in female aged C57BL/6 lacrimal glands.
A. Representative whole histological scans of young and aged female C57BL/6 lacrimal glands stained with H&E. Areas of infiltration are demarcated in dark blue. B. The number of foci (>50 cells) was counted under a 10× microscope lens, and the area of the gland was calculated to generate the focus score on the right. Each dot represents a left lacrimal gland. Kruskal-Wallis with Dunn's multiple comparison test. *P* value as shown. Scale bar = 1000 μm.
C. Representative merged laser scanning confocal microscopy image of young (3-month-old, 3 M) and aged (24-month-old, 24 M) lacrimal glands stained with anti-B220 (green), anti-CD3 (white) and propidium iodide nuclear counterstaining (red). Small insets are magnified. Scale bar 50 μm (left and middle panel) and 10 μm (right panel).
D. Representative immunohistochemistry of aged (26 month-old) lacrimal gland stained with either CD19 or CD3 antibodies (brown color). Scale bar 100 μm.
E. Representative dot plots of CD19 and $B220^+$ stained cells using flow cytometry in lacrimal gland lysates. Cells were gated from $CD45^+$ cells. Numbers in the quadrants represent percent of cells.
F. Accumulative data of frequency of $CD19^+B220^-$, $CD19^+B220^+$ and $CD19^-B220^+$ cells in lacrimal glands. Each dot represents a mouse, $n = 6–10$. Kruskal-Wallis with Dunn's multiple comparison test. *P* value as shown.
G. Relative fold of expression of *Cd19* and *Cd22* in lacrimal gland lysates. Each dot represents a mouse, $n = 8$. Kruskal-Wallis with Dunn's multiple comparison test. P value as shown.

chemoattractant), *Cd5l* (a soluble CD5 ligand with homeostatic effects on B cells [60], *Igkv4–91* (encoding a kappa light chain associated with B cell leukemia marker [61], and *Mzb1* (encoding marginal zone B and B1 cell-specific protein 1) (Fig. 2B) (Supplemental Table 1).

Using the Gene Ontology database, we observed that among the 10 topmost upregulated pathways according to the fold-enrichment score, four pathways were related to antigen processing and presentation by MHC class I and II, two were related to type III hypersensitivity (involving clearance of immune complexes and complement activation), two were related to B cell activation (negative regulation of B cell receptor signaling and toll-like receptor 7 signaling pathways) and one related to elastin catabolic process and one was related to immune complex clearance (Supplemental Fig. 1A). These upregulated pathways are consistent with the development of lymphocytic infiltration in the

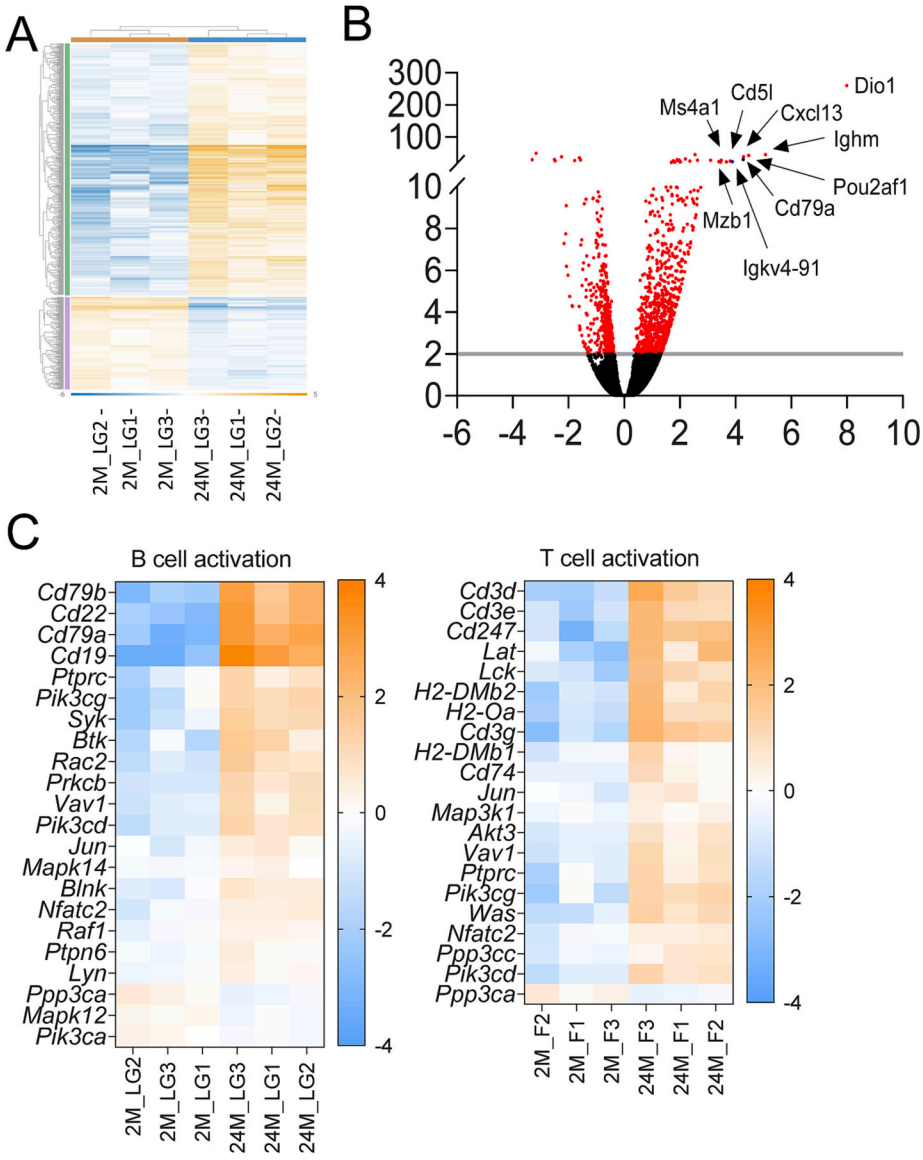

Fig. 2. Increased B cell activation genes in female aged C57BL/6 lacrimal glands.
A. The overall heat map profile for 2220 differentially expressed genes.
B. A volcano plot showing the magnitude of change in the lacrimal gland modulated by aging (Log 1.2-fold change) versus the adjusted *p*-value (−Log10). Some of the most significantly up genes are highlighted. The dotted line indicates a significance of 0.05.
C. Detailed heatmap of significantly differentially expressed genes (DEGs) associated with B and T cell activation.

aged lacrimal glands and chronic inflammation [57]. Downregulated pathways were significantly enriched in DEGs related to "snoRNA guided rRNA pseudouridine synthesis (GO:0000454)," "cytoplasmic translation (GO:0002181)," "ribosomal small subunit assembly (GO:0000028)," "ribosomal large subunit assembly (GO:0000027)" (Supplemental Fig. 1B), suggesting that secretory function of the lacrimal gland is downregulated [62]. Gene ontology related to cellular and molecular processes are shown in the Supplemental Fig. 2.

Pathway analysis using ROSALIND software showed that B cell activation was the topmost upregulated pathway (P adj 4.5e-05), followed by T cell activation (P adj = 0.00032) (Fig. 2C). DEGs involved in B cell activation include transcription factor jun, *Nfatc2*, *Pik3cg*, *Syk*, *Btk and Mapk14 (Mitogen-activated protein kinase 14 or p38alpha)*. Altogether these results indicate that B and T cell pathways and DEGs related to them are the most prevalent in the aging lacrimal gland.

5.3. Increased number of germinal centers in aged lacrimal glands

Germinal centers are organized structures within the B-cell zones of lymphoid tissue where B lymphocytes interact with T cells, proliferate, and undergo somatic hypermutation of their B-cell receptors [63]. Thus, the germinal center response is essential to long-lived, T-cell-dependent humoral immunity. Germinal centers are often found in inflammatory follicles in autoimmunity and chronically inflamed tissues. Since our data in Fig. 1C-D suggested close proximity of B and T cells and gene expression analysis in Fig. 2C showed that B and T cell activation pathways were upregulated in the aged lacrimal gland, we hypothesized that the development of germinal centers could explain these findings, as seen in H&*E*-stained lacrimal gland sections (Fig. 3A). Then, we used flow cytometry to determine the frequency of germinal center related ($CD95^+$ $GL7^+$) B cells in the aged lacrimal gland and ocular draining lymph nodes (dLN) (Fig. 3B). In line with our hypothesis, we observed a progressive increase in the frequency of $CD95^+GL7^+$ cells in both locations, reaching statistical significance at 24 M (Fig. 3C).

Then, we examined our bulk RNAsequencing for DEGs that have been reported to be involved in germinal center formation (Fig. 3D). There was an increase in *Glycam1, Cxcl13* (chemotactic for B cells), *Ltb* (involved in the formation of lymphoid tissue), *Cd274* (encoding PD-L1, an inhibitory factor) and *Cxcl12* (a chemokine involved in B-cell follicle formation). *Glycam1* encodes the Glycam-1 glycoprotein, which is only expressed on high endothelial vessels and by binding to L-selectin allows for leukocyte extravasation to the lymphoid tissue. Using immunostaining, we observed increased immunoreactivity of peripheral node addressin (PNAd, which encompasses Glycam-1) in the aged lacrimal gland (Fig. 3E), a critical step in leukocyte extravasation from vessels. In addition, age-related upregulation of *Glycam1, Cxcl13, Ltb, and Cxcl12* was confirmed by qPCR (Fig. 3F). *Ccl19* and *Ccr7* are also involved in germinal center formation by the stromal cells; although their expression was not upregulated in the bulk RNA sequencing, we demonstrated its increase using individual qPCR reactions with a larger sample size (Fig. 3G). Finally, we observed that B-cell activated factor (BAFF), another critical protein involved in B cell survival encoded by *Tnfsf13b*, progressively increases with aging at mRNA (Fig. 3G) and protein levels (Fig. 3H). CCL21, a chemokine that recruits T cells into lymphoid tissue, was also increased by aging (Fig. 3H). Altogether these results indicate that germinal center-associated transcripts and the frequency of germinal center B cells increase with age in the lacrimal glands.

5.4. Age-related increase in T follicular helper cells

An important feature of germinal centers is the presence of T follicular helper cells, which are responsible for providing the cognate help to B cells required for the development of long-lasting humoral responses [64]. We previously reported an age-related increase in Tfh markers in $CD4^+$ T cells from lymphoid organs in aged mice [11]. Therefore, we investigated if the Tfh markers were increased in aged lacrimal glands. Analyzing the bulk RNAseq data, we observed an increase of *Cxcr5* (encoding the chemokine receptor that allows T cells to enter the B cell areas in lymphoid tissue), *Ly9* (a follicular T cell marker), *Cd84* (crucial for T follicular cell development), *Prdm1* (encoding B lymphocyte–induced maturation protein 1 (Blimp-1), *Il21r* and *Maf* (Fig. 4A). *Maf* activates the promoter and enhancer of *Il21* [65], and in turn, this cytokine and its receptor are critical for germinal center maintenance [66]. We validated the expression of *Cxcr5* and *Il21* by qPCR and flow cytometry. As mice aged, there was a progressive increase in mRNA for *Cxcr5* and *Il21* transcripts in lacrimal glands (Fig. 4B).

Next, we performed flow cytometry in aged lacrimal glands and identified Tfh cells based on the expression of CXCR5, PD-1, BCL-6 (the Tfh master transcription factor), and the signature cytokine IL-21. Cell suspensions from ocular and lacrimal gland draining nodes were used as controls. There was an increase in $CD4^+CXCR5^+PD\text{-}1^+$ cells in the aged lacrimal glands and lymph nodes; however, only aged lacrimal glands had an correspondent increase in $BCL\text{-}6^+IL\text{-}21^+$ cells, characterizing bona fide Tfh cells (Fig. 4C,D).

These results indicate that Tfh cells accumulate with aging inside the lacrimal gland and support our hypothesis that ectopic lymphoid structures develop with aging.

5.5. Marginal zone-like B cells also accumulate with aging

There are three well-defined types of mature B cells: follicular B cells, marginal zone B cells, and B1 cells. Follicular B cells comprise the bulk of germinal centers, whereas B1 cells are more abundant in the peritoneum. Although by definition marginal zone B (MZB) cells are only located at the margin of the T and B cell zones of the spleen, MZB-like cells have been identified in the salivary and lacrimal glands of mice and Sjögren syndrome patients [67,68]. As shown in Fig. 1, we observed an age-related increase in both $CD19^+B220^-$ and $CD19^+B220^+$ cells. Since the latter could potentially correspond to follicular-like B cells and marginal zone B (MZB)-like cells, we quantified the frequency of follicular-like B cells and MZB-like cells based on their differential expression of CD93, IgM and CD23 [69,70]. We only observed a small number of MZB-like cells ($B220^+CD93^-IgM^+CD23^-$) and follicular-like B cells ($B220^+CD93^-IgM^+CD23^+$) in the lacrimal glands of young mice. In comparison, eye-draining lymph nodes from young mice had a higher frequency of follicular B cells (Fig. 5A,B). The frequency of MZB-like and follicular-like B cells in lacrimal glands increased as mice aged (Fig. 5A, B). There was also a significant increase in MZB-like cells in aged draining lymph nodes.

Infiltration of MZB-like cells in salivary and lacrimal glands has been previously reported in Sjögren syndrome [68,69,71]. We then investigated in our bulk RNA sequencing the genes related to MZB cells that have been reported in Sjögren syndrome salivary glands, since this is the most characterized gland in the disease. In line with the flow cytometry data, there was an upregulation of DEGs involved in MZB cell signal transduction and receptor ligands, integrins, chemokine, chemokine receptors, and Rho-GTP family members and pathways (Fig. 5C). Altogether these results indicate that MZB-like cells accumulate in the lacrimal glands as mice age and this is accompanied by an upregulation of transcripts related to their activation.

5.6. Isotype switch and local antibody production in the aged lacrimal gland

One feature of germinal centers is local production of antibodies by plasma cells. It is well established that tears are rich in secretory IgA, a critical immunoglogulin in mucosal tissues [72,73]. To assess if there was a local production of immunoglobulins, we stained young and lacrimal glands using antibodies for B220 and IgA, IgD, IgM and IgG1 (Fig. 6A). Young lacrimal glands showed minimal reactivity to IgD, IgG1 and IgM, but IgA^+ cells were present, in agreement with the literature. In aged lacrimal glands, there was an increase in IgD^+, IgM^+ and IgG^+ cells.

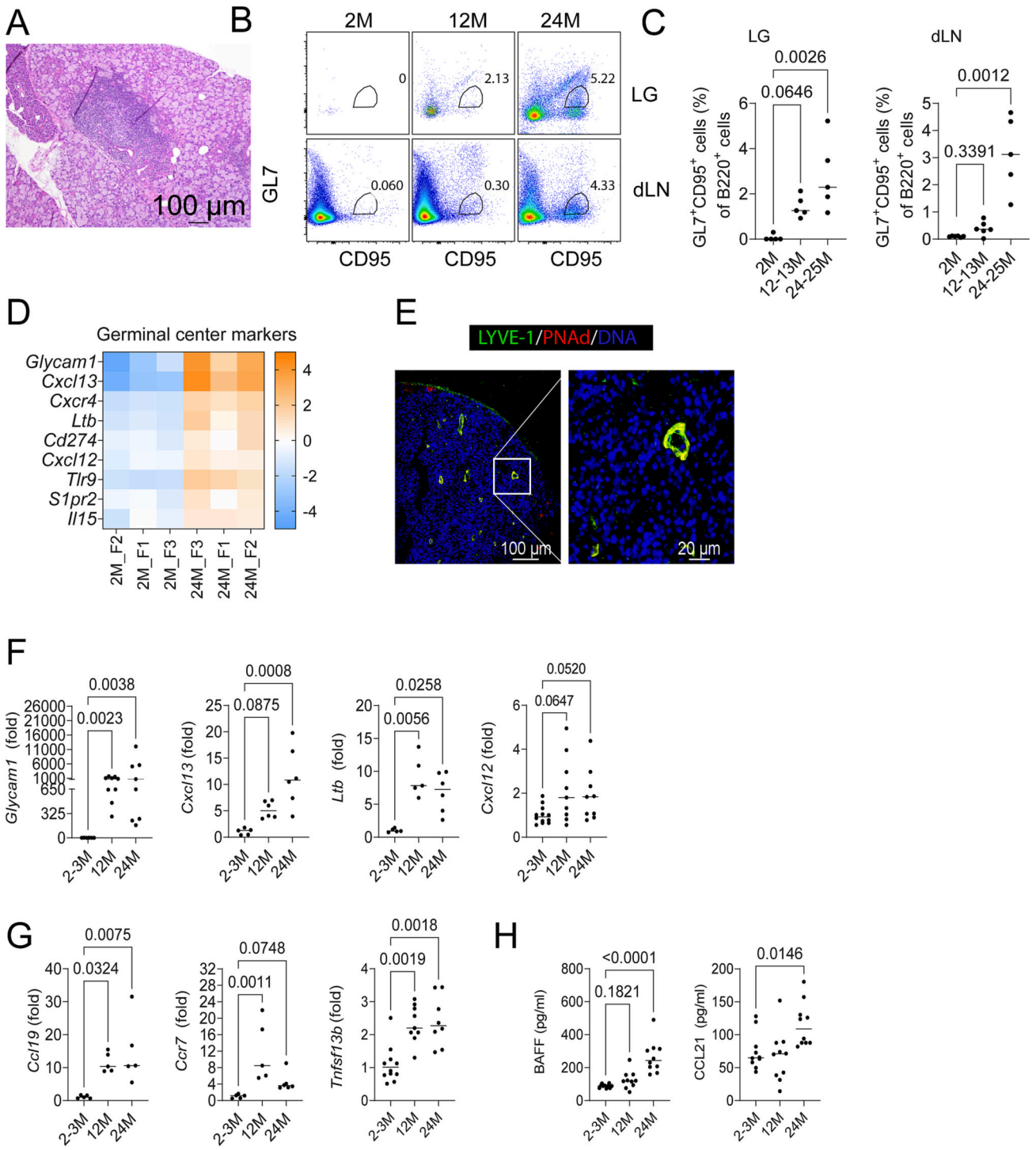

Fig. 3. Germinal center in female aged C57BL/6 lacrimal glands.

A. Representative H&E of an aged lacrimal gland (LG) showing germinal-center like infiltration. Scale bar = 50 µm.

B. Representative dot plots of the lacrimal gland (LG) and draining lymph nodes (dLN) suspensions stained with GL7 and CD95. Cells were gated as described in the methods.

C. Accumulative data of frequency of $GL7^{+}CD95^{+}$ cells in lacrimal glands (LG) and draining lymph nodes (dLN). Each dot represents a mouse, $n = 5$. Kruskal-Wallis with Dunn's multiple comparison test. *P* value as shown.

D. Heatmaps showing DEG related to germinal center formation.

E. Representative merged laser scanning confocal microscopy image of aged (24-month-old, 24 M) lacrimal glands stained with anti-LYVE-1 (green), PNAd (red), and DAPI counterstaining (blue). Scale bar 100 µm (left) and 20 µm (right panel).

F-G. Relative fold of expression of *Glycam1, Cxcl13, Ltb, Cxcl12* (F) *and Cccl19, Ccr7, Tnfsf13b* (G) in lacrimal gland lysates determined by qPCR. Each dot represents a mouse, $n = 8$. Kruskal-Wallis with Dunn's multiple comparison test. P value as shown.

H. Luminex assay showing protein levels of BAFF and CCL21. Each dot represents a mouse, n = 8. Kruskal-Wallis with Dunn's multiple comparison test. P value as shown.

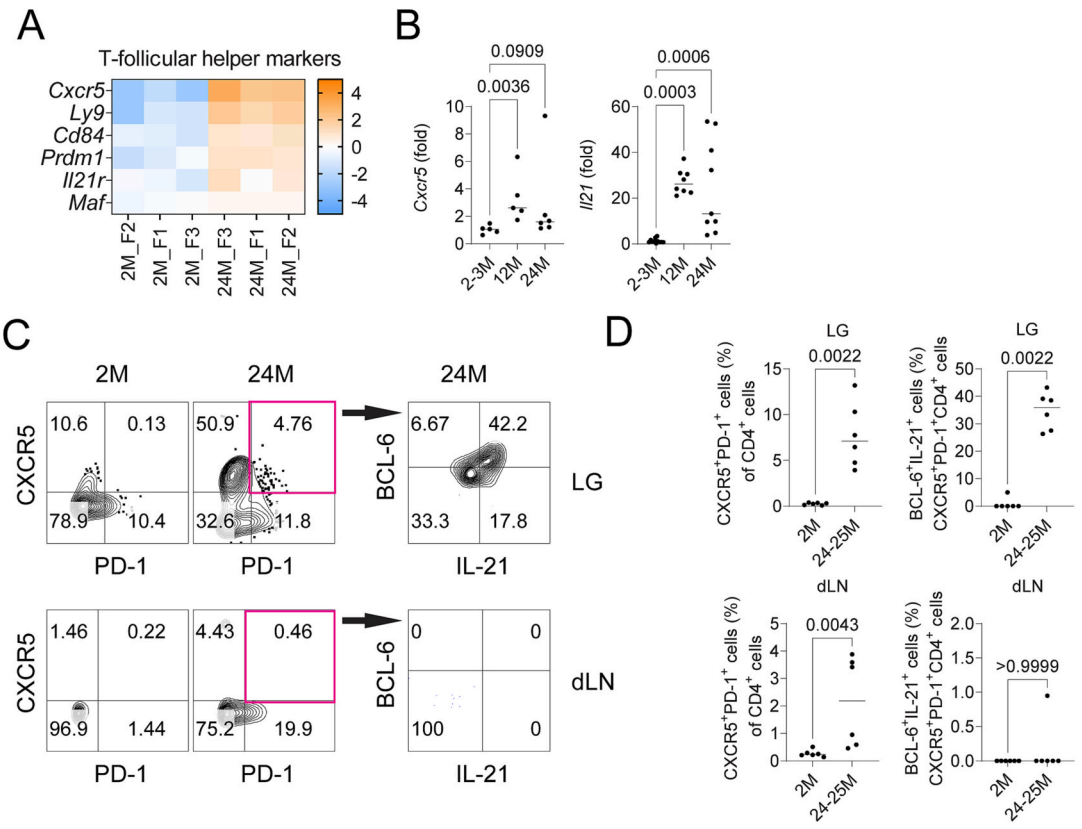

Fig. 4. Age-related increased frequency of T follicular helper cells in female C57BL/6 lacrimal glands.
A. Heatmaps showing DEG related to Tfh markers.
B. Relative fold expression of *Cxcr5, Il21* in lacrimal gland lysates. Each dot represents a mouse, $n = 8–10$. Kruskal-Wallis with Dunn's multiple comparison test. P value as shown.
C. Representative density plots of CXCR5 and PD-1 were further gated into BCL6 and IL-21 in single-cell suspensions of the lacrimal gland (LG) and draining lymph nodes (dLN).
D. Accumulative data of $CXCR5^+PD\text{-}1^+$ cells and $BCL\text{-}6^+IL\text{-}21^+$ cells in lacrimal gland and dLN. Each dot represents a mouse, n = 8. Kruskal-Wallis with Dunn's multiple comparison test. P value as shown.

IgD^+ $B220^+$ B cells were easily identified while IgM and IgG^+ cells were B220 negative, suggestive of plasma cells. Of note, some IgM^+ and $IgG1^+$ cells were in close contact with deposits of autofluorescent material suggestive of lipofuscin (Fig. 6A).

Next, we segregated the genes related to all immunoglobulins (Fig. 6B) and observed that although only *Ighm* (encoding IgM) reached statistical significance using FDR, several other immunoglobulin genes were also upregulated. We also investigated plasma cell-related markers (Fig. 6C) and observed upregulation of 19 genes and downregulation of 4 genes related to plasma cell biology. Of note, among the upregulated genes were *Tnfrsf17* (receptor for B-cell activating factor), which is crucial for plasma cell survival, and *Tnfrsf13b* (receptor for B-cell activating factor -BAFF- and a proliferation inducing ligand -APRIL-), which promotes isotype switch and terminal differentiation of B cells to plasma cells [74]. Finally, numerous immunoglobulin kappa-light and heavy chain variable genes were differentially upregulated in lacrimal glands with aging, indicating the polyclonal nature of the infiltrating B cells and/or plasma cells. Altogether these findings indicate that in the aged lacrimal gland, the increasing numbers of infiltrating B cells undergo isotype switch and differentiate into plasma cells that produce antibodies *in situ*.

5.7. Effects of diversity background on ectopic lymphoid structures

The B6 mice are the most used mouse strain in aging studies. Overall, the B6 mice are Th1/Th17 prone [75,76] and they might not represent the breadth of immune responses in the elderly mice. To understand the consequences of a diverse genetic background (as it exists in humans) on age-related dry eye, we investigated the age-related lacrimal gland phenotype in the Diversity Outbred mice (Jackson Labs, Bar Harbor, ME). The diversity outbred parental lines (the collaborative cross strains) were developed by crossing eight unique and genetically diverse inbred mouse strains (A/J, B6, 129S1/SvImJ, NOD/ShiLtJ, NZO/HlLtJ, CAST/EiJ, PWK/PhJ, and WSB/EiJ), followed by subsequent inbreeding to produce new and unique recombinant incipient inbred lines. Analysis of young and aged diversity outbred mice showed that immune infiltrates are more prominent in the lacrimal gland of aged female diversity outbred mice (Fig. 7A-B), while age-related goblet cell loss is similar in both sexes (Fig. 7C). These results indicate that the presence of ectopic lymphoid structures in the lacrimal glands is not restricted to a single mouse strain.

5.8. Shared and unique pathways in lacrimal glands of aged and Sjögren syndrome model mice

Sjögren syndrome is an autoimmune disease that affects the exocrine glands, causing dry eye and mouth. One pathognomic feature of Sjögren syndrome is the immune cell infiltration of salivary and lacrimal glands. Another pathognomonic sign is the presence of autoantibodies in the sera, such as SS-A and SS-B autoantibodies. Aging is another example of dysregulated immunity that has many signs of autoimmunity, including immune infiltration as described in this study, but also increased levels of autoantibodies [77–80]. Using commercially available ELISAs [81], we measured the levels of anti-Ro52/SS-A and anti-La/SS-B

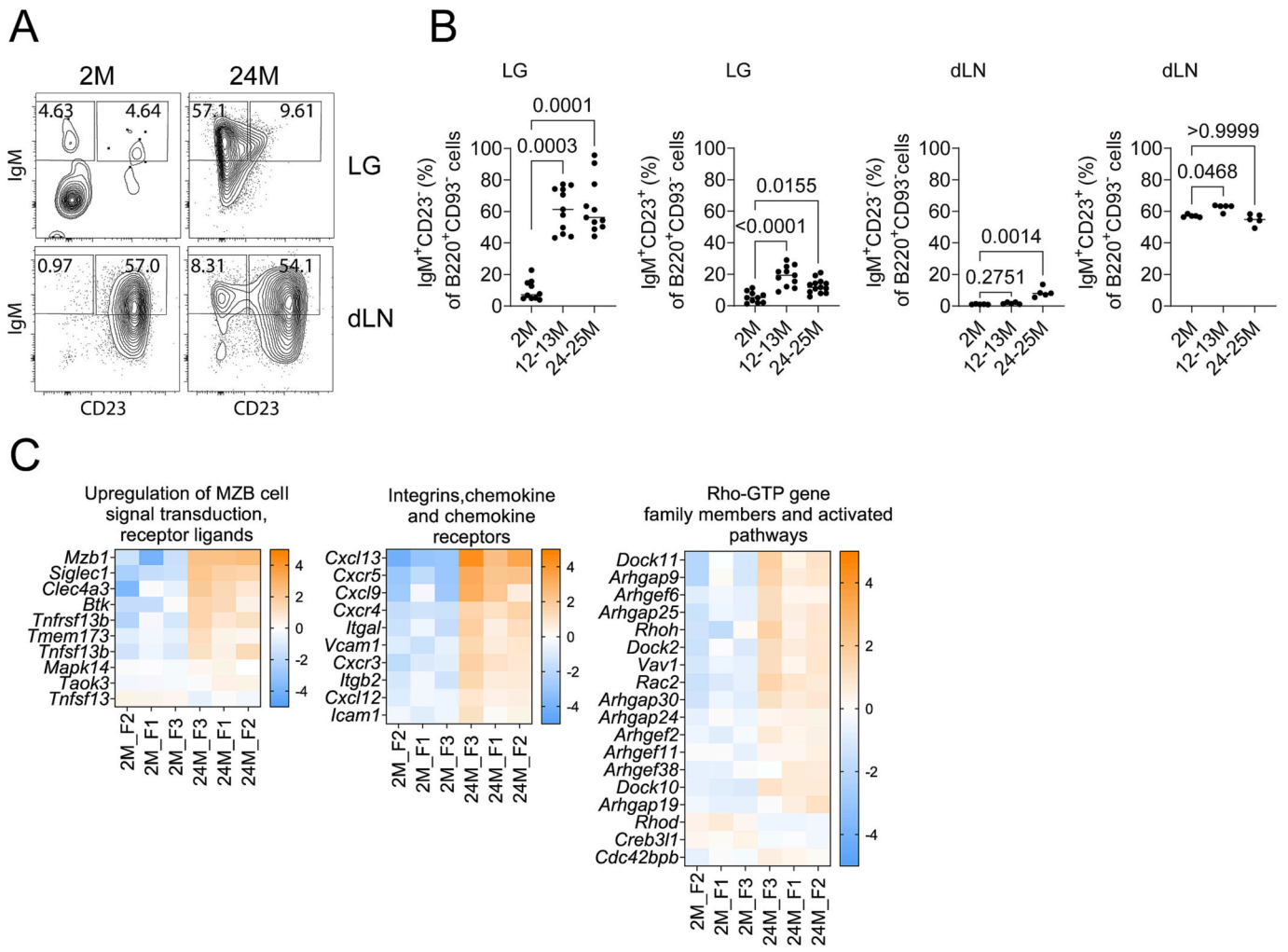

Fig. 5. Age-related increase in marginal zone-like B cells in female C57BL/6 lacrimal glands.
A. Representative density plots of IgM and CD23 cells in single cell suspensions of lacrimal glands (LG) and draining lymph nodes. Cells were gated sequentially as $CD45^+$, $B220^+CD93^-$ cells and then IgM and CD23 were plotted.
B. Accumulative data of $CD93^-IgM^+CD23^-$ (MZB) and $CD93^-IgM^+CD23^+$ (FO) cells. Each dot represents a mouse, n = 8. Kruskal-Wallis with Dunn's multiple comparison test. P value as shown.
C. Heatmaps showing DEGs related to MZB cell biology.

autoantibodies in the sera of mice of different ages. Increased levels of anti-SS-A and anti-SS-B autoantibodies were observed in 12-13 M and remained elevated by 24 M.

To gain insights into common and unique pathways between Sjögren syndrome and aging, we performed a meta-analysis of the DEGs previously obtained (1) by comparing young with aged lacrimal glands, and (2) by comparing control BALB/c with the non-obese diabetic mice (NOD.B10.$H2^b$), a primary Sjögren syndrome model that also develops B and T cell infiltrates forming ectopic lymphoid structures in the lacrimal gland [39]. We obtained 12 DEG expression patterns (**P**) noted from **P1** to **P12**) (Fig. 9, Supplemental Table 2) and sorted them into 3 main groups: DEGs following the same trend in both datasets (Fig. 9A), DEGs altered specifically in Sjögren syndrome (Fig. 9B), and DEGs following opposite trends between aging and Sjögren syndrome (Fig. 9C).

In the first series of consistent patterns between the two datasets (Fig. 9A), we found many upregulated biological pathways (in **P1, P2, P3, P4, P5**) related to the adaptive immune response, leukocyte activation, and cytokine production. They included genes expressed by B cells (MHC class II molecules and immunoglobulins), T cells (*Cd27*), and myeloid lineages (*Aif1, Cd80, Cd86*). This was expected since the activation of the innate response and the appearance of lymphocytic infiltrates are common features of both conditions. Most of the average fold changes for DEGs of these pathways were higher in the NOD.B10.$H2^b$/BALBc comparison, thus illustrating a greater activation of inflammatory processes in the Sjögren syndrome mouse model compared to aging. For example, cathepsin S has been implicated in Sjögren syndrome and aging [39,82–85]. We observed that although cathepsin S was upregulated in both datasets (**P4**, Fig. 8A), it was higher in the Sjögren syndrome group (NOD.B10.$H2^b$ vs BALBc at 4 M: FC = 5.45; p-adj = 1.40e-34) than during aging (24 M vs 2 M: FC = 3.38; p-adj = 2.28e-26).

Although both data sets shared a set of downregulated genes (P6 and P7, Fig. 9A), the downregulation of genes related to "cytoplasmic ribosomal proteins", "formation of ternary complex" and "mRNA processing" (**P6**) suggesting a reduced secretory function was more important in aged than in NOD.B10.$H2^b$ lacrimal glands. By contrast, we found that DEGs of pattern **P7** were more downregulated in Sjögren syndrome lacrimal glands compared to aged glands. They were enriched in "cell morphogenesis" (**P7**), which included several transcription factors involved in cell signaling and differentiation *Etv1* (FGF responsive gene, which is consistent with the lack of lacrimal gland repair), *Six4* (regulates germline and somatic cell migration and also nerve development/regeneration) as well as receptors for growth factors (*Fgfr1, Erbb2*, *Met*). We also found "regulation of synapse structure or activity", which is

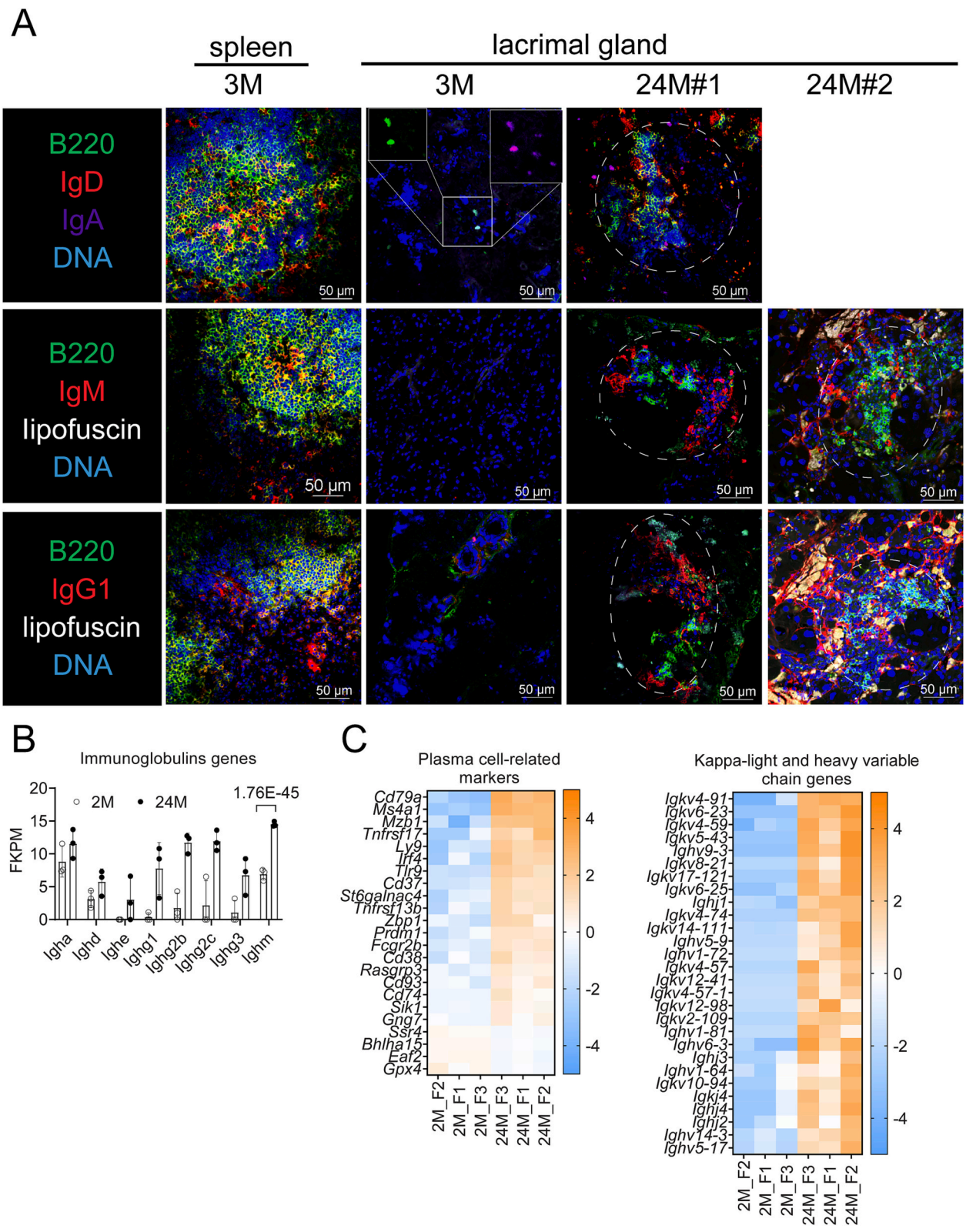

Fig. 6. Increased immunoglobulin production in female aged C57BL/6 lacrimal glands.

A. Merged images of laser confocal microscopy of spleen and lacrimal glands from 3-month (3 M) and 24-month-old (24 M) stained with B220 (green) and different immunoglobulin isotype antibodies as shown. Square insets in the top row show B220 and IgA single staining. In the second and third rows, there is autofluorescence at the margins of the infiltrates; this has been described as lipofuscin inclusions. Areas of infiltrates in aged lacrimal glands are demarcated by dotted ellipse. Scale bar = 50 um.

B. Normalized raw counts (fragments per million, FKPM) of immunoglobulin genes from bulk RNA Sequencing. *p* value indicates FDR from ROSALIND® software, calculated as described in the "Methods."

C. Heatmaps showing DEGs related to plasma cells (D) and kappa and variable chain.

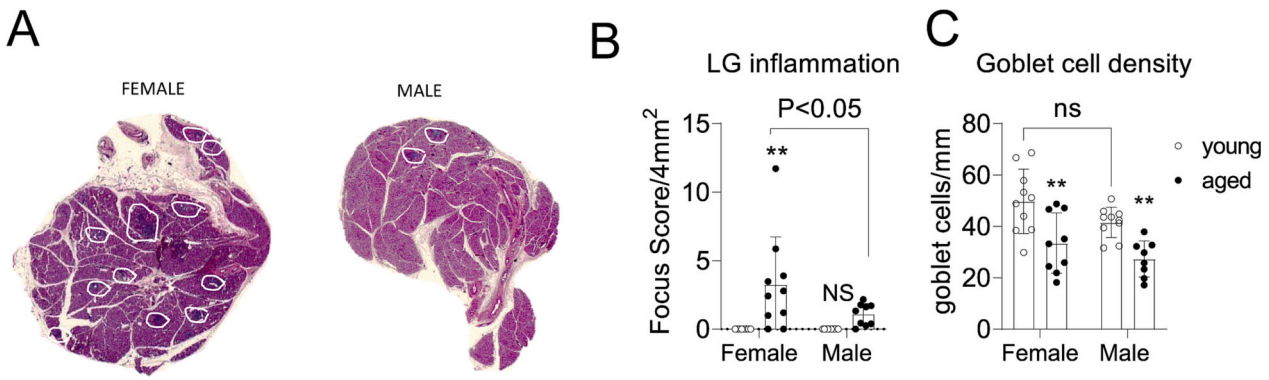

Fig. 7. Aged diversity outbred mice display lacrimal gland infiltration and goblet cell loss.
A. Representative scans of whole H&E-stained lacrimal glands of the aged female and male diversity outbred mice. Areas of infiltration are demarcated in white.
B. Accumulative data of focus score/4mm^2 as a measurement of lacrimal gland infiltration (left panel).
C. Accumulative data of goblet cell density in diversity outbred mice in young (3–4 months) and aged (23–25-months age). Each dot represents one mouse, $n = 10$/age/group. Kruskal-Wallis with Dunn's multiple comparison test.

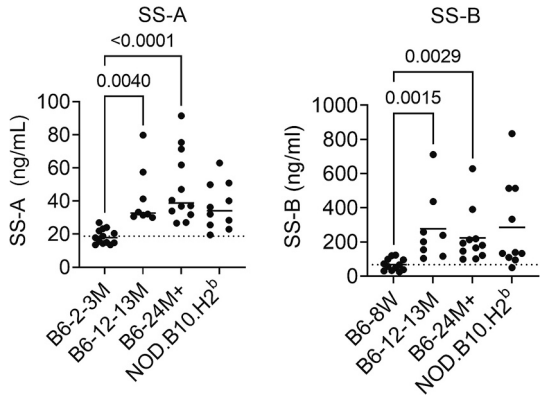

Fig. 8. Increased anti-Ro52/SS-A and anti-la/SS-B antibodies in the sera of aged female C57BL/6 mice.
Serum was collected from female C57BL/6 (B6) mice of different ages. Male sera from NOD.B10.H2^b mice (which develop dacryoadenitis) were used as positive controls. Each dot represents one animal. Kruskal-Wallis with Dunn's multiple comparison test, n = 8–14/group. Dotted line indicates mean of young control group.

consistent with the alteration/destruction of lacrimal gland innervation, and "monocarboxylic acid metabolic process" that contained genes involved in lipid metabolism (*Acadl, Cpt1a, Ppara, Rxra*).

The second series of patterns were specific to NOD.B10.H2^b mice (Fig. 9B). The fact that "immunoglobulin production" was enriched in both upregulated (**P5**: *Ighd,* numerous *Igkv* genes) and downregulated (**P9**: *Igkv4* and *Igkv8* segments) gene lists of Sjögren syndrome suggests that variable segments are differentially modulated during the disease. Genes involved in the cell cycle and mitosis were specifically upregulated in Sjögren syndrome lacrimal glands (**P8**). They are likely induced by actively proliferating lymphocytes present in the lymphoid follicles developing in the lacrimal gland of NOD·H-2^b mice.

The third series of patterns showed opposite gene expression changes during aging and Sjögren syndrome-like disease (Fig. 9C). Some of the genes related to cell division upregulated during Sjögren syndrome were downregulated in aged lacrimal glands (**P10**) and rather suggest impaired lacrimal gland repair/cell proliferation. Aged lacrimal glands were also characterized by the upregulation of genes expressed by fibroblasts and forming or remodeling the extracellular matrix (metalloproteinase, collagens), genes involved in angiogenesis ("tube morphogenesis") and genes belonging to signaling pathways activated by tyrosine receptor kinases (*Fgf10, Fgfr2, Igf1, Pdgfra*) (**P12**). This suggests that fibrotic processes activated by fibroblasts are specific to aging. On the other hand, we found a strong decrease in the expression of genes involved in Wnt signaling and the metabolism of amino acids and NADPH in the Sjögren syndrome group (**P11**), thus suggesting a reduced metabolic activity in NOD.B10.H2^b lacrimal glands.

In sum, the main alteration shared by aging and Sjögren syndrome mice is the upregulation of the pro-inflammatory processes leading to the recruitment of leukocytes into the lacrimal gland and the formation of ectopic lymphoid structures. By contrast, mitotic, metabolic and fibrotic processes are differentially altered between the two models.

6. Discussion

With aging comes immune dysregulation and the increased onset of autoimmunity. As a result, there is a higher prevalence of dry eye and Sjögren syndrome in the elderly [58,86,87], although the underlying mechanisms are not fully understood. Here we show that aging is associated with the appearance of ectopic lymphoid tissue in the lacrimal glands of mice. We observed that B and T cells increasingly infiltrate the lacrimal glands with age, developing into follicular structures with germinal centers and T follicular cells. Although we published before that aged lacrimal glands have an influx of B cells, the results of our study show a significant heterogeneity of these cells. We found an increase in CD19$^+$B220$^-$ cells, putatively identified as B1 cells, in agreement with the literature [3]. However, the majority of B220$^+$ cells were CD19$^+$ cells, indicating presence of mature B cells. We further characterized these cells and observed an increase in cells found in germinal centers. Intriguingly, we also detected MZB-like B cells in the aged lacrimal gland. Moreover, gene expression analysis of aged lacrimal glands evidenced increased B cell activation and interaction between T and B cells, suggestive of functional immune responses or tertiary lymphoid tissue formation. Gene expression analysis of aged and Sjögren syndrome lacrimal glands revealed that despite the many biological pathways in common, age-related dysregulation and Sjögren syndrome are two distinct entities. Finally, these findings were confirmed in genetically diverse mice to rule out strain-specific effects.

There is a definitive body of evidence showing that *ex vivo* measurements of protein levels after agonist stimulation are decreased in aged lacrimal glands compared to young [88–92]. Although profound changes are seen in the aged lacrimal glands of mice (such as those shown in Fig. 1), many groups (including us) have reported a paradoxical increase in tear volume with aging and in inflammatory conjunctival diseases as measured by the cotton thread test or Schirmer strips [43,93–95]. However, aged mice are larger than young mice, and when tear volume was normalized by body mass, the ration between tear volume and body mass stayed constant [54]. These finding indicates

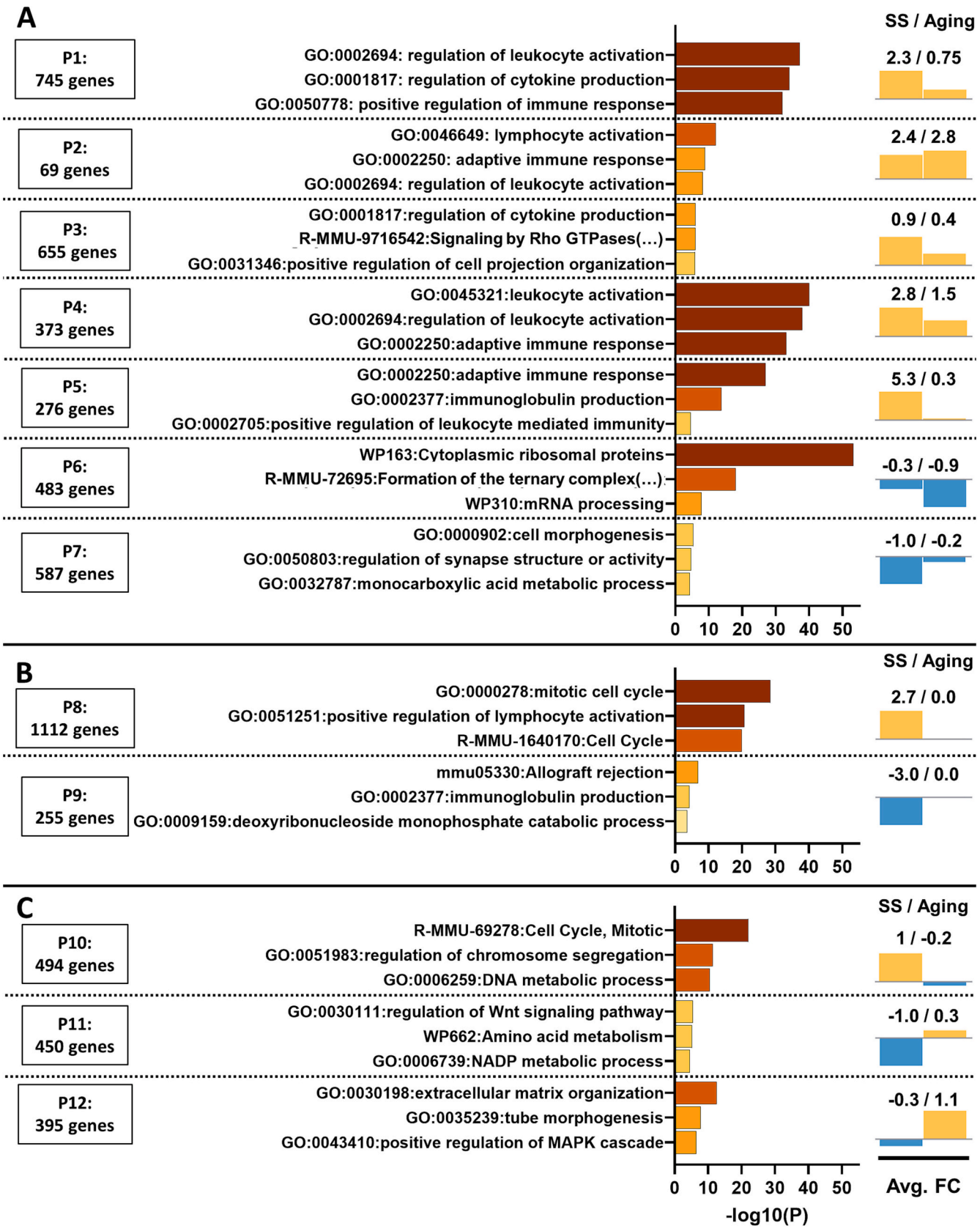

Fig. 9. Meta-analysis showing shared and unique pathways in Sjögren syndrome and aged lacrimal glands.
Meta-analysis comparing RNAseq of Sjögren syndrome (SS) and aging datasets. 12 different patterns of expression have been obtained and divided into 3 categories: (A) DEGs upregulated or downregulated in both datasets, (B) DEGs altered specifically in SS and (C) DEGs differentially regulated between Aging and SS. -Log10(*P*-value) of Top-3 pathways enriched by these genes have been plotted. On the right, a summary of gene expression for that pattern is shown to indicate its trend (upregulated in yellow, downregulated in blue) and its Average Fold Change (Avg. FC) in each dataset.

that tear volume measurements at the tear meniscus might not be the best measure of lacrimal gland function *in vivo* in aged mice. Alternatively, measurement of pro-inflammatory cytokines may offer a better option to investigate lacrimal gland involvement with aging and it can be performed in live animals.

The appearance of ectopic lymphoid tissue, known as lymphoid neogenesis, is associated with non-resolving, persistent inflammation and, more importantly, is often a harbinger of autoimmunity [96]. Progress has been made in our knowledge of the initial events in the development of ectopic lymphoid tissue. Experimental models show that eliciting inflammation in the exocrine glands of mice by local adenovirus injection [97] or inducing lacrimal gland expression of lymphotoxins α/β (LTA/LTB) leads to its appearance [98]. In line with this, we found upregulated *Ltb* in aged lacrimal glands in this study, and the numerous proinflammatory changes that occur with aging in the lacrimal gland have been reviewed recently [54]. We have previously shown that aged lacrimal glands have increased expression of TNF-α and IL-17 [11,24], two critical mediators in ectopic lymphoid tissue formation in other tissues [97]. In line with the importance of TNF-α in ectopic lymphoid structures [14], we also showed that *Tnf*$^{-/-}$ mice had decreased age-related ectopic lymphoid structures [99]. Another cytokine implicated in tertiary lymphoid organ appearance is IL-22 [100], but it was not upregulated in our sets of data. Once initiated, the development of ectopic lymphoid tissue is sustained by several chemokine/chemokine receptor pathways, namely CXCL13/CXCR5, CCL19-CCL21/CCR7, and CXCL12/CXCR4, which attract more B and T cells [96,101]. Of note, all these genes were upregulated in aged lacrimal glands. *Cxcl13* transcripts showed a progressive age-related increase, while *Ccl19*, *Ccr7*, *Cxcl12* and *Ltb* showed elevated middle-age levels maintained at 24 months. Another feature of established ectopic lymphoid tissue we observed in the aged lacrimal glands is the presence of peripheral node addressin-expressing high-endothelial venules. These specialized blood vessels allow for the extravasation of circulating naïve and central memory T cells in response to the locally produced CCL19-CCL21 chemokine gradient to initiate adaptive immune responses *in situ* [102].

Multiple findings in our study support the notion of increasingly functional ectopic lymphoid structures in the aged lacrimal glands. The growing presence of T follicular cells (Fig. 4), the upregulated B-cell activation pathways (Fig. 2), and the growing number of germinal centers (Fig. 3) indicate that a local humoral response develops with aging in the lacrimal gland. Consistently, we also observed upregulation of plasma cell-related genes (Fig. 6C), IgM, and a positive trend for different IgG subtypes (Fig. 6B). In particular, the upregulation of plasma cell survival-related genes suggests that the aged lacrimal gland becomes a favorable niche for long-lasting plasma cells [103], similarly to findings in the salivary glands in Sjögren syndrome [104,105]. Of note, we have previously reported increased immunoglobulin levels in aged tears [106] which agrees with this data. While we did not validate individual immunoglobulin genes using qPCR, it is possible that these immunoglobulins would be differentially expressed in aged lacrimal glands if we had a larger sample size. Extranodal B cell lymphoma in lacrimal glands has been reported [107–111] and may present as oligoclonality of the infiltrating B cells. Our findings, however, indicate polyclonality in the infiltrating B cells and plasma cells and support the notion of antigen-specific humoral responses developing locally in the aged lacrimal gland.

Perhaps the most intriguing finding of our study is the age-related influx of MZB-like cells in the lacrimal gland. MZB cells express polyreactive B cell receptors, which typically bind multiple epitopes on pathogens and apoptotic cells with low affinity and are readily stimulated by their pattern recognition receptors [67]. Thus, MZB cells are ideally poised to act as the first responders to infections with a quick production of neutralizing polyreactive antibodies, but they are also prone to autoimmunity. In particular, the observation of MZB cells outside the spleen is linked to autoimmune disease [67]. In Sjögren syndrome-susceptible mice, an early wave of MZB-like cells infiltrate the salivary glands before the onset of the T cell-dependent immune response that drives gland destruction [39,71]. In another murine model of arthritis, MZB cells act as efficient antigen-presenting cells due to their polyreactivity and thus activate self-reactive CD4^{+} T cells, which in turn provide the required help to autoreactive follicular B cells that produce highly specific antibodies [112]. Thus, it is possible that infiltration of the aging lacrimal gland with MZB cells sets the stage for ectopic lymphoid structures and potentially autoimmunity, as we also observed an upregulation of genes linked to MZB signal transduction in the aged lacrimal gland (Fig. 5C). Of note, with aging comes a dysregulation of MZB cells in mice [113].

Contrasting our knowledge of the formation of ectopic lymphoid structures, its implications in the aged lacrimal gland are less understood. Lymphoid neogenesis in other tissues may occur as part of an antigen-dependent immune response, as is the case for several autoimmune disorders, or in an antigen-independent fashion as a nonspecific reaction to chronic inflammation [114]. Aging brings about oxidative stress and inflammation [24,54], and in line with this, we previously reported that modulating the Nrf2 transcription factor, which controls the expression of antioxidant and detoxification genes, leads to a reduction in lacrimal gland lymphoid infiltration [24]. This result, however, does not rule out the possibility of autoimmune-driven lymphoid tissue formation nor it excludes a potentially increased susceptibility to autoimmunity in the aged lacrimal gland. In Sjögren syndrome, ectopic lymphoid tissue is associated with disease severity [115,116]. In animal models of Sjögren syndrome, blockade of ectopic lymphoid structures using the LTβ receptor IgG (murine receptor fused to mouse IgG1) in the NOD mouse improved salivary gland function and decreased the number of inflammatory cytokines and immune infiltrates [117–119]. It also decreased the influx of naive cells into salivary and lacrimal glands [120]. Mice expressing LTα/β in the salivary and lacrimal glands develop ectopic lymphoid tissue but this is insufficient to induce humoral autoimmunity [98]. However, these mice have an early decrease in tear flow and atrophic lacrimal glands, suggesting that increased ectopic lymphoid structures might be detrimental to lacrimal gland [98] However, the effects of similar interventions in aged lacrimal gland have not yet been investigated.

Ectopic lymphoid structures formation in the aged lacrimal gland resembles the pathological findings in primary Sjögren syndrome [115], an auto-immune condition characterized by exacerbated inflammation of exocrine organs, auto-autoimmune B cell activation and sicca syndrome. Salivary glands of primary Sjögren syndrome patients have increased presence of ectopic lymphoid structures. The relationship between ectopic lymphoid structures and disease progression in primary Sjögren syndrome is still debated but the presence of these structures correlates with aberrant B cell activation and the presence of systemic autoantibodies [121–123]. Similarly, aged mice showed increased levels of autoantibodies in our studies, in agreement with the literature [77–80]. The concentration levels were in the range observed in autoimmune NOD.B10.H2^{b} mice, which are well known to develop SS-A and SS-B autoantibodies [121–123]. Lymphocytic infiltration of the lacrimal and salivary glands is also more frequent in Sjögren syndrome patients with poor reflex tearing [124]. In this context, primary Sjögren syndrome might represent the tip of the iceberg from an inflammatory and auto-immune-driven process in exocrine glands. Our gene expression analysis comparison showed that aging and Sjögren syndrome have many shared molecular pathways (mostly related to the activation of the immune system), albeit at different levels. While aging showed specific modulation of certain pathways, it is also possible that our snapshot investigation might have missed alterations yet to be developed. For example, DEGs related to fibrosis were upregulated in the aging but not in the Sjögren syndrome glands; however, biopsies of human minor salivary glands are accompanied by significant fibrosis. Whether ectopic lymphoid structures in the exocrine glands from aged individuals and primary Sjögren syndrome patients are triggered by the same mechanisms or if they are composed by the same type of immune cells is not

known and future research is warranted to understand the contributions of these ectopic lymphoid structures to the health of aging lacrimal glands.

Supplementary data to this article can be found online at https://doi.org/10.1016/j.clim.2023.109251.

Contributions

CSdP: conceptualization, data curation, formal analysis, funding acquisition, investigation, methodology, project administration, resources, writing (original draft and review and editing). JGG: formal analysis, funding acquisition, investigation, methodology, writing (original draft, review and editing). KKS, CMT-V, ZY, OM, VD, HPM: methodology, validation, formal analysis, writing (review and editing).

Support

This work was supported by the National Institutes of Health/National Eye Institute (NEI) R01EY030447 (CSdP), EY-002520 (Center Core Grant for Vision Research, Core Grant for Vision Research Department of Ophthalmology at Baylor College of Medicine), NEI Training Grant in Vision Sciences T32 EY007001 (KKS); 5R01EY026202 (HPM) and National Institute of Dental and Craniofacial Research (NIDCR) grant R01DE031044 (HPM), Research to Prevent Blindness (Dept. of Ophthalmology), The Hamill Foundation, The Sid Richardson Foundation, and by Baylor College of Medicine Pathology Core (NCI P30CA125123). Jeremias Galletti received a Fulbright Visiting Scholar Award to participate in this study and he is funded by Wellcome Trust 221859/Z/20/Z and Agencia Nacional de Promoción Científica y Tecnológica (Argentina, PICT 2018–02911, PICT 2020–00138). Claudia M. Trujillo-Vargas received supplemental salary support from Facultad de Medicina, Universidad de Antioquia, UdeA, Medellin, Colombia. This project was supported by the Cytometry and Cell Sorting Core at Baylor College of Medicine with funding from the NIH (CA125123 and RR024574) and from a CPRIT Core facility Support Award (RP180672), and the expert assistance of Joel M. Sederstrom.

The funders had no role in the design and conduct of the study; collection, management, analysis, and interpretation of the data; preparation, review, or approval of the manuscript; and decision to submit the manuscript for publication.

Declaration of Competing Interest

CSDP was a consultant to Spring Discovery from May to August 2022. All other authors declare no conflicts of interest.

Data availability

Data will be made available on request. The datasets for this study can be found in the GEO repository (Access ID GSE224596).

Acknowledgments

We gratefully acknowledge the contribution of Leiqi Zhang to the management of the aged colony and Kevin Tesareski for the histology preparation.

References

[1] C.S. de Paiva, A.J. St Leger, R.R. Caspi, Mucosal immunology of the ocular surface, Mucosal Immunol. (2022) 1–15.
[2] E. Knop, N. Knop, Lacrimal drainage-associated lymphoid tissue (LDALT): a part of the human mucosal immune system, Invest. Ophthalmol. Vis. Sci. 42 (2001) 566–574.
[3] W. Saitoh-Inagawa, T. Hiroi, M. Yanagita, H. Iijima, E. Uchio, S. Ohno, K. Aoki, H. Kiyono, Unique characteristics of lacrimal glands as a part of mucosal immune network: high frequency of IgA-committed B-1 cells and NK1.1+ alphabeta T cells, Invest. Ophthalmol. Vis. Sci. 41 (2000) 138–144.
[4] O.G. Gudmundsson, H. Benediktsson, K. Olafsdottir, T-lymphocyte subsets in the human lacrimal gland, Acta Ophthalmol. 66 (1988) 19–23.
[5] O.G. Gudmundsson, J. Bjornsson, K. Olafsdottir, K.J. Bloch, M.R. Allansmith, D. A. Sullivan, T cell populations in the lacrimal gland during aging, Acta Ophthalmol. 66 (1988) 490–497.
[6] R. Wieczorek, F.A. Jakobiec, E.H. Sacks, D.M. Knowles, The immunoarchitecture of the normal human lacrimal gland. Relevancy for understanding pathologic conditions, Ophthalmology 95 (1988) 100–109.
[7] M. Segerberg-Konttinen, Focal adenitis in lacrimal and salivary glands. A post-mortem study, Scand. J. Rheumatol. 17 (1988) 379–385.
[8] B.E. Damato, D. Allan, S.B. Murray, W.R. Lee, Senile atrophy of the human lacrimal gland: the contribution of chronic inflammatory disease, Br. J. Ophthalmol. 68 (1984) 674–680.
[9] H. Obata, S. Yamamoto, H. Horiuchi, R. Machinami, Histopathologic study of human lacrimal gland. Statistical analysis with special reference to aging, Ophthalmology 102 (1995) 678–686.
[10] M. Nasu, O. Matsubara, H. Yamamoto, Post-mortem prevalence of lymphocytic infiltration of the lacrymal gland: a comparative study in autoimmune and non-autoimmune diseases, J. Pathol. 143 (1984) 11–15.
[11] C.M. Trujillo-Vargas, K.E. Mauk, H. Hernandez, R.G. de Souza, Z. Yu, J. G. Galletti, J. Dietrich, F. Paulsen, C.S. de Paiva, Immune phenotype of the CD4+ T cells in the aged lymphoid organs and lacrimal glands, GeroScience 44 (4) (2022) 2105–2128, https://doi.org/10.1007/s11357-022-00529-z.
[12] F. Perros, P. Dorfmüller, D. Montani, H. Hammad, W. Waelput, B. Girerd, N. Raymond, O. Mercier, S. Mussot, S. Cohen-Kaminsky, M. Humbert, B. N. Lambrecht, Pulmonary lymphoid neogenesis in idiopathic pulmonary arterial hypertension, Am. J. Respir. Crit. Care Med. 185 (2012) 311–321.
[13] E. Pipi, S. Nayar, D.H. Gardner, S. Colafrancesco, C. Smith, F. Barone, Tertiary lymphoid structures: autoimmunity goes local, Front. Immunol. (2018) 9.
[14] M.M. Ligon, C. Wang, E.N. DeJong, C. Schulz, D.M.E. Bowdish, I.U. Mysorekar, Single cell and tissue-transcriptomic analysis of murine bladders reveals age- and TNFα-dependent but microbiota-independent tertiary lymphoid tissue formation, Mucosal Immunol. 13 (2020) 908–918.
[15] S. Chotikavanich, C.S. de Paiva, J.J. Chen, F. Bian, W.J. Farley, S.C. Pflugfelder, Production and activity of matrix Metalloproteinase-9 on the ocular surface increase in dysfunctional tear syndrome, Invest. Ophthalmol. Vis. Sci. 50 (2009) 3203–3209.
[16] S.C. Pflugfelder, C.S. De Paiva, Q.L. Moore, E.A. Volpe, D.Q. Li, K. Gumus, M. L. Zaheer, R.M. Corrales, Aqueous tear deficiency increases conjunctival interferon-γ (IFN-γ) expression and goblet cell loss, Invest. Ophthalmol. Vis. Sci. 56 (2015) 7545–7550.
[17] S.C. Pflugfelder, R.M. Corrales, C.S. de Paiva, T helper cytokines in dry eye disease, Exp. Eye Res. 117 (2013) 118–125.
[18] G. Goverse, B.J. Olivier, R. Molenaar, M. Knippenberg, M. Greuter, T. Konijn, E. C. Cook, M.R. Beijer, D.M. Fedor, J.M. den Haan, J.L. Napoli, G. Bouma, R. E. Mebius, Vitamin a metabolism and mucosal immune function are distinct between BALB/c and C57BL/6 mice, Eur. J. Immunol. 45 (2015) 89–100.
[19] S. Nasseri, B. Nikkho, S. Parsa, A. Ebadifar, F. Soleimani, K. Rahimi, Z. Vahabzadeh, M.B. Khadem-Erfan, J. Rostamzadeh, B. Baban, O. Banafshi, V. Assadollahi, S. Mirzaie, F. Fathi, Generation of Fam83h knockout mice by CRISPR/Cas9-mediated gene engineering, J. Cell. Biochem. 120 (7) (2019) 11033–11043, https://doi.org/10.1002/jcb.28381.
[20] National Research Council Committee for the Update of the Guide for the C, Use of Laboratory a: The National Academies Collection: Reports Funded by National Institutes of Health. Guide for the Care and Use of Laboratory Animals, National Academy of Sciences, Washington (DC), 2011. National Academies Press (US) Copyright © 2011.
[21] S.E. Moss, R. Klein, B.E. Klein, Prevalence of and risk factors for dry eye syndrome, ArchOphthalmol 118 (2000) 1264–1268.
[22] D.A. Schaumberg, D.A. Sullivan, J.E. Buring, M.R. Dana, Prevalence of dry eye syndrome among US women, Am J. Ophthalmol. 136 (2003) 318–326.
[23] E.A. Volpe, J.T. Henriksson, C. Wang, F.L. Barbosa, M. Zaheer, X. Zhang, S. C. Pflugfelder, C.S. de Paiva, Interferon-gamma deficiency protects against aging-related goblet cell loss, Oncotarget 7 (2016) 64605–66461.
[24] R.G. de Souza, Z. Yu, H. Hernandez, C.M. Trujillo-Vargas, A. Lee, K.E. Mauk, J. Cai, M.R. Alves, C.S. de Paiva, Modulation of oxidative stress and inflammation in the aged lacrimal gland, Am. J. Pathol. 191 (2020) 294–308.
[25] C.S. de Paiva, A.L. Villarreal, R.M. Corrales, H.T. Rahman, V.Y. Chang, W. J. Farley, M.E. Stern, J.Y. Niederkorn, D.Q. Li, S.C. Pflugfelder, Dry eye-induced conjunctival epithelial squamous metaplasia is modulated by interferon-{gamma}, Invest. Ophthalmol. Vis. Sci. 48 (2007) 2553–2560.
[26] C.S. de Paiva, R.M. Corrales, A.L. Villarreal, W. Farley, D.Q. Li, M.E. Stern, S. C. Pflugfelder, Apical corneal barrier disruption in experimental murine dry eye is abrogated by methylprednisolone and doxycycline, Invest. Ophthalmol. Vis. Sci. 47 (2006) 2847–2856.
[27] J.D. Rios, Y. Horikawa, L.L. Chen, C.L. Kublin, R.R. Hodges, D.A. Dartt, D. Zoukhri, Age-dependent alterations in mouse exorbital lacrimal gland structure, innervation and secretory response, Exp. Eye Res. 80 (2005) 477–491.
[28] M. Martin, Cutadapt removes adapter sequences from high-throughput sequencing reads, EMBnetjournal 17 (2011) 10–12.
[29] A. Dobin, C.A. Davis, F. Schlesinger, J. Drenkow, C. Zaleski, S. Jha, P. Batut, M. Chaisson, T.R. Gingeras, STAR: ultrafast universal RNA-seq aligner, Bioinformatics 29 (2013) 15–21.
[30] S. Anders, P.T. Pyl, W. Huber, HTSeq—a Python framework to work with high-throughput sequencing data, Bioinformatics 31 (2015) 166–169.

[31] M.I. Love, W. Huber, S. Anders, Moderated estimation of fold change and dispersion for RNA-seq data with DESeq2, Genome Biol. 15 (2014) 550.
[32] L. Wang, S. Wang, W. Li, RSeQC: quality control of RNA-seq experiments, Bioinformatics 28 (2012) 2184–2185.
[33] A. Alexa, J. R: topGO: Enrichment Analysis for Gene Ontology. R Package Version 1381, 2019.
[34] A.L. Mitchell, T.K. Attwood, P.C. Babbitt, M. Blum, P. Bork, A. Bridge, S. D. Brown, H.Y. Chang, S. El-Gebali, M.I. Fraser, J. Gough, D.R. Haft, H. Huang, I. Letunic, R. Lopez, A. Luciani, F. Madeira, A. Marchler-Bauer, H. Mi, D. A. Natale, M. Necci, G. Nuka, C. Orengo, A.P. Pandurangan, T. Paysan-Lafosse, S. Pesseat, S.C. Potter, M.A. Qureshi, N.D. Rawlings, N. Redaschi, L.J. Richardson, C. Rivoire, G.A. Salazar, A. Sangrador-Vegas, C.J.A. Sigrist, I. Sillitoe, G.G. Sutton, N. Thanki, P.D. Thomas, S.C.E. Tosatto, S.Y. Yong, R.D. Finn, InterPro in 2019: improving coverage, classification and access to protein sequence annotations, Nucleic Acids Res. 47 (2019) D351–d60.
[35] L.Y. Geer, A. Marchler-Bauer, R.C. Geer, L. Han, J. He, S. He, C. Liu, W. Shi, S. H. Bryant, The NCBI BioSystems database, Nucleic Acids Res. 38 (2010) D492–D496.
[36] A. Subramanian, P. Tamayo, V.K. Mootha, S. Mukherjee, B.L. Ebert, M.A. Gillette, A. Paulovich, S.L. Pomeroy, T.R. Golub, E.S. Lander, J.P. Mesirov, Gene set enrichment analysis: a knowledge-based approach for interpreting genome-wide expression profiles, Proc. Natl. Acad. Sci. U. S. A. 102 (2005) 15545–15550.
[37] A. Fabregat, S. Jupe, L. Matthews, K. Sidiropoulos, M. Gillespie, P. Garapati, R. Haw, B. Jassal, F. Korninger, B. May, M. Milacic, C.D. Roca, K. Rothfels, C. Sevilla, V. Shamovsky, S. Shorser, T. Varusai, G. Viteri, J. Weiser, G. Wu, L. Stein, H. Hermjakob, P. D'Eustachio, The Reactome pathway knowledgebase, Nucleic Acids Res. 46 (2018) D649–d55.
[38] D.N. Slenter, M. Kutmon, K. Hanspers, A. Riutta, J. Windsor, N. Nunes, J. Mélius, E. Cirillo, S.L. Coort, D. Digles, F. Ehrhart, P. Giesbertz, M. Kalafati, M. Martens, R. Miller, K. Nishida, L. Rieswijk, A. Waagmeester, L.M.T. Eijssen, C.T. Evelo, A. R. Pico, E.L. Willighagen, WikiPathways: a multifaceted pathway database bridging metabolomics to other omics research, Nucleic Acids Res. 46 (2018) D661–d7.
[39] O. Mauduit, V. Delcroix, T. Umazume, C.S. de Paiva, D.A. Dartt, H. P. Makarenkova, Spatial transcriptomics of the lacrimal gland features macrophage activity and epithelium metabolism as key alterations during chronic inflammation, Front. Immunol. 13 (2022) 1011125.
[40] O.D. Schein, M.C. Hochberg, B. Munoz, J.M. Tielsch, K. Bandeen-Roche, T. Provost, G.J. Anhalt, S. West, Dry eye and dry mouth in the elderly: a population-based assessment, Arch. Intern. Med. 159 (1999) 1359–1363.
[41] O.D. Schein, B. Munoz, J.M. Tielsch, K. Bandeen-Roche, S. West, Prevalence of dry eye among the elderly, Am J. Ophthalmol. 124 (1997) 723–728.
[42] A.J. Bron, C.S. de Paiva, S.K. Chauhan, S. Bonini, E.E. Gabison, S. Jain, E. Knop, M. Markoulli, Y. Ogawa, V. Perez, Y. Uchino, N. Yokoi, D. Zoukhri, D.A. Sullivan, TFOS DEWS II pathophysiology report, Ocul. Surf. 15 (3) (2017) 438–510, https://doi.org/10.1016/j.jtos.2017.05.011.
[43] A.J. McClellan, E.A. Volpe, X. Zhang, G.J. Darlington, D.Q. Li, S.C. Pflugfelder, C. S. de Paiva, Ocular surface disease and dacryoadenitis in aging C57BL/6 mice, Am. J. Pathol. 184 (2014) 631–643.
[44] C.J. Nien, J.R. Paugh, S. Massei, A.J. Wahlert, W.W. Kao, J.V. Jester, Age-related changes in the meibomian gland, Exp. Eye Res. 89 (2009) 1021–1027.
[45] C.J. Nien, S. Massei, G. Lin, C. Nabavi, J. Tao, D.J. Brown, J.R. Paugh, J.V. Jester, Effects of age and dysfunction on human meibomian glands, Arch. Ophthalmol. 129 (2011) 462–469.
[46] G.J. Parfitt, Y. Xie, M. Geyfman, D.J. Brown, J.V. Jester, Absence of ductal hyper-keratinization in mouse age-related meibomian gland dysfunction (ARMGD), Aging 5 (2013) 825–834.
[47] M.A. Stepp, S. Pal-Ghosh, G. Tadvalkar, A. Williams, S.C. Pflugfelder, C.S. de Paiva, Reduced intraepithelial corneal nerve density and sensitivity accompany desiccating stress and aging in C57BL/6 mice, Exp. Eye Res. 169 (2018) 91–98.
[48] J. He, T.L. Pham, H.E.P. Bazan, Neuroanatomy and neurochemistry of rat cornea: changes with age, The Ocular Surf 20 (2020) 86–94, https://doi.org/10.1016/j.jtos.2020.11.005.
[49] S.S. Tummanapalli, M.D.P. Willcox, T. Issar, N. Kwai, A.M. Poynten, A. V. Krishnan, J. Pisarcikova, M. Markoulli, The effect of age, gender and body mass index on tear film Neuromediators and corneal nerves, Curr. Eye Res. 45 (2020) 411–418.
[50] M.E.H. De Silva, L.J. Hill, L.E. Downie, H.R. Chinnery, The effects of aging on corneal and ocular surface homeostasis in mice, Invest. Ophthalmol. Vis. Sci. 60 (2019) 2705–2715.
[51] F. Bian, Y. Xiao, F.L. Barbosa, R.G. de Souza, H. Hernandez, Z. Yu, S. C. Pflugfelder, C.S. de Paiva, Age-associated antigen-presenting cell alterations promote dry-eye inducing Th1 cells, Mucosal Immunol. 12 (2019) 897–908.
[52] S.B. Aronson, M.B. Fish, M. Pollycove, M.A. Coon, Altered vascular permeability in ocular inflammatory disease, Arch. Ophthalmol. 85 (1971) 455–466.
[53] C.M. Trujillo-Vargas, S. Kutlehria, H. Hernandez, R.G. de Souza, A. Lee, Z. Yu, S. C. Pflugfelder, M. Singh, C.S. de Paiva, Rapamycin Eyedrops increased CD4(+) Foxp3(+) cells and prevented goblet cell loss in the aged ocular surface, Int. J. Mol. Sci. (2020) 21.
[54] R.G. de Souza, C.S. de Paiva, M.R. Alves, Age-related autoimmune changes in lacrimal glands, Immune Net. 19 (2019), e3.
[55] Y. Sato, P. Boor, S. Fukuma, B.M. Klinkhammer, H. Haga, O. Ogawa, J. Floege, M. Yanagita, Developmental stages of tertiary lymphoid tissue reflect local injury and inflammation in mouse and human kidneys, Kidney Int. 98 (2020) 448–463.
[56] P. Singh, Z.Z. Coskun, C. Goode, A. Dean, L. Thompson-Snipes, G. Darlington, Lymphoid neogenesis and immune infiltration in aged liver, Hepatology 47 (2008) 1680–1690.
[57] T. Umazume, W.M. Thomas, S. Campbell, H. Aluri, S. Thotakura, D. Zoukhri, H. P. Makarenkova, Lacrimal gland inflammation deregulates extracellular matrix remodeling and alters molecular signature of epithelial stem/progenitor cells, Invest. Ophthalmol. Vis. Sci. 56 (2015) 8392–8402.
[58] J.G. Galletti, C.S. de Paiva, The ocular surface immune system through the eyes of aging, Ocul. Surf. 20 (2021) 139–162.
[59] C. Zhao, J. Inoue, I. Imoto, T. Otsuki, S. Iida, R. Ueda, J. Inazawa, POU2AF1, an amplification target at 11q23, promotes growth of multiple myeloma cells by directly regulating expression of a B-cell maturation factor, TNFRSF17, Oncogene 27 (2008) 63–75.
[60] R. Fenutría, V.G. Martinez, I. Simões, J. Postigo, V. Gil, M. Martínez-Florensa, J. Sintes, R. Naves, K.S. Cashman, J. Alberola-Ila, M. Ramos-Casals, G. Soldevila, C. Raman, J. Merino, R. Merino, P. Engel, F. Lozano, Transgenic expression of soluble human CD5 enhances experimentally-induced autoimmune and anti-tumoral immune responses, PLoS One 9 (2014), e84895.
[61] S. Iacovelli, E. Hug, S. Bennardo, M. Duehren-von Minden, S. Gobessi, A. Rinaldi, M. Suljagic, D. Bilbao, G. Bolasco, J. Eckl-Dorna, V. Niederberger, F. Autore, S. Sica, L. Laurenti, H. Wang, R.J. Cornall, S.H. Clarke, C.M. Croce, F. Bertoni, H. Jumaa, D.G. Efremov, Two types of BCR interactions are positively selected during leukemia development in the Eμ-TCL1 transgenic mouse model of CLL, Blood 125 (2015) 1578–1588.
[62] K. Mizuta, J.R. Warner, Continued functioning of the secretory pathway is essential for ribosome synthesis, Mol. Cell. Biol. 14 (1994) 2493–2502.
[63] M. Stebegg, S.D. Kumar, A. Silva-Cayetano, V.R. Fonseca, M.A. Linterman, L. Graca, Regulation of the germinal center response, Front. Immunol. 9 (2018) 2469.
[64] C.S. Ma, E.K. Deenick, M. Batten, S.G. Tangye, The origins, function, and regulation of T follicular helper cells, J. Exp. Med. 209 (2012) 1241–1253.
[65] Y. Hiramatsu, A. Suto, D. Kashiwakuma, H. Kanari, S.-I. Kagami, K. Ikeda, K. Hirose, N. Watanabe, M.J. Grusby, I. Iwamoto, H. Nakajima, c-Maf activates the promoter and enhancer of the IL-21 gene, and TGF-β inhibits c-Maf-induced IL-21 production in CD4+ T cells, J. Leukoc. Biol. 87 (2010) 703–712.
[66] M.A. Linterman, L. Beaton, D. Yu, R.R. Ramiscal, M. Srivastava, J.J. Hogan, N. K. Verma, M.J. Smyth, R.J. Rigby, C.G. Vinuesa, IL-21 acts directly on B cells to regulate Bcl-6 expression and germinal center responses, J. Exp. Med. 207 (2010) 353–363.
[67] A.E. Palm, S. Kleinau, Marginal zone B cells: from housekeeping function to autoimmunity? J. Autoimmun. 119 (2021), 102627.
[68] N. Singh, I. Chin, P. Gabriel, E. Blaum, S. Masli, Dysregulated marginal zone B cell compartment in a mouse model of Sjögren's syndrome with ocular inflammation, Int. J. Mol. Sci. 19 (2018) 3117.
[69] L. Shen, C. Gao, L. Suresh, Z. Xian, N. Song, L.D. Chaves, M. Yu, J.L. Ambrus Jr., Central role for marginal zone B cells in an animal model of Sjogren's syndrome, Clin. Immunol. 168 (2016) 30–36.
[70] V. Gies, D. Bouis, M. Martin, J.L. Pasquali, T. Martin, A.S. Korganow, P. Soulas-Sprauel, Phenotyping of autoreactive B cells with labeled nucleosomes in 56R transgenic mice, Sci. Rep. 7 (2017) 13232.
[71] A.B. Peck, C.Q. Nguyen, J. Ambrus, Early covert appearance of marginal zone B cells in salivary glands of Sjögren's syndrome-susceptible mice: initiators of subsequent overt clinical disease, Int. J. Mol. Sci. (2021) 22.
[72] A.J. Macpherson, B. Yilmaz, J.P. Limenitakis, S.C. Ganal-Vonarburg, IgA function in relation to the intestinal microbiota, Annu. Rev. Immunol. 36 (2018) 359–381.
[73] B.L. Horwitz, G.R. Christensen, S.R. Ritzmann, Diurnal profiles of tear lysozyme and gamma a globulin, AnnOphthalmol (1978) 75–80.
[74] S.L. Kalled, C. Ambrose, Y.M. Hsu, The biochemistry and biology of BAFF, APRIL and their receptors, Curr. Dir. Autoimmun. 8 (2005) 206–242.
[75] L.D. Hazlett, S. McClellan, B. Kwon, R. Barrett, Increased severity of Pseudomonas aeruginosa corneal infection in strains of mice designated as Th1 versus Th2 responsive, Invest. Ophthalmol. Vis. Sci. 41 (2000) 805–810.
[76] H. Watanabe, K. Numata, T. Ito, K. Takagi, A. Matsukawa, Innate immune response in TH1- and TH2-dominant mouse strains, Shock 22 (2004).
[77] J.J. Goronzy, C.M. Weyand, Immune aging and autoimmunity, Cell. Mol. Life Sci. : CMLS 69 (2012) 1615–1623.
[78] Y. Hayashi, M. Utsuyama, C. Kurashima, K. Hirokawa, Spontaneous development of organ-specific autoimmune lesions in aged C57BL/6 mice, Clin. Exp. Immunol. 78 (1989) 120–126.
[79] M. Faderl, F. Klein, O.F. Wirz, S. Heiler, L. Albertí-Servera, C. Engdahl, J. Andersson, A. Rolink, Two distinct pathways in mice generate antinuclear antigen-reactive B cell repertoires, Front. Immunol. 9 (2018), 16.
[80] A. Nusser, N. Nuber, O.F. Wirz, H. Rolink, J. Andersson, A. Rolink, The development of autoimmune features in aging mice is closely associated with alterations of the peripheral CD4(+) T-cell compartment, Eur. J. Immunol. 44 (2014) 2893–2902.
[81] A. Suzuki, C. Iwaya, K. Ogata, H. Yoshioka, J. Shim, I. Tanida, M. Komatsu, N. Tada, J. Iwata, Impaired GATE16-mediated exocytosis in exocrine tissues causes Sjögren's syndrome-like exocrinopathy, Cell. Mol. Life Sci. : CMLS 79 (2022) 307.
[82] Z. Yu, J. Li, G. Govindarajan, S.F. Hamm-Alvarez, J. Alam, D.Q. Li, C.S. de Paiva, Cathepsin S is a novel target for age-related dry eye, Exp. Eye Res. 214 (2021), 108895.
[83] S.F. Hamm-Alvarez, S.R. Janga, M.C. Edman, S. Madrigal, M. Shah, S. E. Frousiakis, K. Renduchintala, J. Zhu, S. Bricel, K. Silka, D. Bach, M. Heur, S. Christianakis, D.G. Arkfeld, J. Irvine, W.J. Mack, W. Stohl, Tear cathepsin S as a

candidate biomarker for Sjogren's syndrome, Arthritis & Rheumatol. (Hoboken, NJ) 66 (2014) 1872–1881.
[84] W. Klinngam, S.R. Janga, C. Lee, Y. Ju, F. Yarber, M. Shah, H. Guo, D. Wang, J. A. MacKay, M.C. Edman, S.F. Hamm-Alvarez, Inhibition of Cathepsin S reduces lacrimal gland inflammation and increases tear flow in a mouse model of Sjogren's syndrome, Sci. Rep. 9 (2019) 9559.
[85] E. Jobs, E. Ingelsson, U. Risérus, E. Nerpin, M. Jobs, J. Sundström, S. Basu, A. Larsson, L. Lind, J. Ärnlöv, Association between serum Cathepsin S and mortality in older adults, JAMA 306 (2011) 1113–1121.
[86] K. Whaley, J. Williamson, T. Wilson, D.D. McGavin, G.R. Hughes, H. Hughes, L. R. Schmulian, R.N. MacSween, W.W. Buchanan, Sjogren's syndrome and autoimmunity in a geriatric population, Age Ageing 1 (1972) 197–206.
[87] A.A. Drosos, A.P. Andonopoulos, J.S. Costopoulos, C.S. Papadimitriou, H. M. Moutsopoulos, Prevalence of primary Sjögren's syndrome in an elderly population, Br. J. Rheumatol. 27 (1988) 123–127.
[88] C.E. Draper, J. Singh, E. Adeghate, Effects of age on morphology, protein synthesis and secretagogue-evoked secretory responses in the rat lacrimal gland, Mol. Cell. Biochem. 248 (2003) 7–16.
[89] C.E. Draper, E.A. Adeghate, J. Singh, D.J. Pallot, Evidence to suggest morphological and physiological alterations of lacrimal gland acini with ageing, Exp. Eye Res. 68 (1999) 265–276.
[90] C.E. Draper, E. Adeghate, P.A. Lawrence, D.J. Pallot, A. Garner, J. Singh, Age-related changes in morphology and secretory responses of male rat lacrimal gland, J. Auton. Nerv. Syst. 69 (1998) 173–183.
[91] B.B. Bromberg, M.H. Welch, Lacrimal protein secretion: comparison of young and old rats, Exp. Eye Res. 40 (1985) 313–320.
[92] B.B. Bromberg, M.M. Cripps, M.H. Welch, Sympathomimetic protein secretion by young and aged lacrimal gland, Curr. Eye Res. 5 (1986) 217–223.
[93] I.C. You, F. Bian, E.A. Volpe, C.S. de Paiva, S.C. Pflugfelder, Age-related conjunctival disease in the C57BL/6.NOD-Aec1Aec2 mouse model of Sjogren syndrome develops independent of lacrimal dysfunction, Invest. Ophthalmol. Vis. Sci. 56 (2015) 2224–2233.
[94] I. Alcalde, A. Inigo-Portugues, O. Gonzalez-Gonzalez, L. Almaraz, E. Artime, C. Morenilla-Palao, J. Gallar, F. Viana, J. Merayo-Lloves, C. Belmonte, Morphological and functional changes in TRPM8-expressing corneal cold thermoreceptor neurons during aging and their impact on tearing in mice, J. Comp. Neurol. 526 (2018) 1859–1874.
[95] C.K. Marko, B.B. Menon, G. Chen, J.A. Whitsett, H. Clevers, I.K. Gipson, Spdef null mice lack conjunctival goblet cells and provide a model of dry eye, AmJPathol 183 (2013) 35–48.
[96] E. Corsiero, A. Nerviani, M. Bombardieri, C. Pitzalis, Ectopic lymphoid structures: powerhouse of autoimmunity, Front. Immunol. 7 (2016) 430.
[97] M. Bombardieri, F. Barone, D. Lucchesi, S. Nayar, W.B. van den Berg, G. Proctor, C.D. Buckley, C. Pitzalis, Inducible tertiary lymphoid structures, autoimmunity, and exocrine dysfunction in a novel model of salivary gland inflammation in C57BL/6 mice, J. Immunol. 189 (2012) 3767–3776.
[98] L.A. Truman, K.L. Bentley, N.H. Ruddle, Lymphotoxin targeted to salivary and lacrimal glands induces tertiary lymphoid organs and cervical lymphadenopathy and reduces tear production, Eur. J. Immunol. 50 (2020) 418–425.
[99] C.S. De Paiva, E.N. DeJong, A. Lee, K.E. Mauk, D.M.E. Bowdish, A. I. Sindikubwabo, R. Korstanje, Z. Yu, H.P. Makarenkova, Effects of age, TNF-α and calorie restriction on cathepsin S and other inflammatory markers in the lacrimal gland, Invest. Ophthalmol. Vis. Sci. 62 (2021) 2045.
[100] F. Barone, S. Nayar, J. Campos, T. Cloake, D.R. Withers, K.M. Toellner, Y. Zhang, L. Fouser, B. Fisher, S. Bowman, J. Rangel-Moreno, L. Garcia-Hernandez Mde, T. D. Randall, D. Lucchesi, M. Bombardieri, C. Pitzalis, S.A. Luther, C.D. Buckley, IL-22 regulates lymphoid chemokine production and assembly of tertiary lymphoid organs, Proc. Natl. Acad. Sci. U. S. A. 112 (2015) 11024–11029.
[101] F. Barone, M. Bombardieri, A. Manzo, M.C. Blades, P.R. Morgan, S. J. Challacombe, G. Valesini, C. Pitzalis, Association of CXCL13 and CCL21 expression with the progressive organization of lymphoid-like structures in Sjogren's syndrome, Arthritis Rheum. 52 (2005) 1773–1784.
[102] T. Into, S. Niida, K.-I. Shibata, MyD88 signaling causes autoimmune sialadenitis through formation of high endothelial venules and upregulation of LTβ receptor-mediated signaling, Sci. Rep. 8 (2018) 14272.
[103] S.M. Lightman, A. Utley, K.P. Lee, Survival of long-lived plasma cells (LLPC): piecing together the puzzle, Front. Immunol. 10 (2019) 965.
[104] K. Skarstein, J.L. Jensen, H. Galtung, R. Jonsson, K. Brokstad, L.A. Aqrawi, Autoantigen-specific B cells and plasma cells are prominent in areas of fatty infiltration in salivary glands of patients with primary Sjögren's syndrome, Autoimmunity 52 (2019) 242–250.
[105] E.A. Szyszko, K.A. Brokstad, G. Oijordsbakken, M.V. Jonsson, R. Jonsson, K. Skarstein, Salivary glands of primary Sjögren's syndrome patients express factors vital for plasma cell survival, Arthritis Res. & Therap. 13 (2011) R2.
[106] J.G. Galletti, M. Guzman, M.N. Giordano, Mucosal immune tolerance at the ocular surface in health and disease, Immunology 150 (2017) 397–407.
[107] C.S. Chean, V. Sovani, A. Boden, C. Knapp, Lacrimal gland extranodal marginal zone B-cell lymphoma in the presence of amyloidosis, Orbit 41 (2022) 350–353.
[108] A. Grixti, S.E. Coupland, J. Hsuan, Lacrimal gland extranodal marginal zone B-cell lymphoma of mucosa-associated lymphoid tissue-type associated with massive amyloid deposition, Acta Ophthalmol. 94 (2016) e667–e668.
[109] Y.C. Lin, H.C. Kau, S.C. Kao, W.M. Hsu, C.C. Tsai, Systemically disseminated extranodal marginal zone B-cell lymphoma of lacrimal gland in a patient with systemic lupus erythematosus, Ophthalmic Plast. Reconstr. Surg. 23 (2007) 72–73.
[110] S.C. Kao, H.C. Kau, C.C. Tsai, S.H. Tsay, C.F. Yang, J.S. Wu, W.M. Hsu, Lacrimal gland extranodal marginal zone B-cell lymphoma of MALT-type, Am J. Ophthalmol. 143 (2007) 311–316.
[111] S.E. Coupland, M. Hellmich, C. Auw-Haedrich, W.R. Lee, I. Anagnostopoulos, H. Stein, Plasmacellular differentiation in extranodal marginal zone B cell lymphomas of the ocular adnexa: an analysis of the neoplastic plasma cell phenotype and its prognostic significance in 136 cases, Br. J. Ophthalmol. 89 (2005) 352–359.
[112] C. Carnrot, K.E. Prokopec, K. Rasbo, M.C. Karlsson, S. Kleinau, Marginal zone B cells are naturally reactive to collagen type II and are involved in the initiation of the immune response in collagen-induced arthritis, Cell. Mol. Immunol. 8 (2011) 296–304.
[113] V.M. Turner, N.A. Mabbott, Ageing adversely affects the migration and function of marginal zone B cells, Immunology 151 (2017) 349–362.
[114] S. Fleig, T. Kapanadze, J. Bernier-Latmani, J.K. Lill, T. Wyss, J. Gamrekelashvili, D. Kijas, B. Liu, A.M. Hüsing, E. Bovay, A.C. Jirmo, S. Halle, M. Ricke-Hoch, R. H. Adams, D.R. Engel, S. von Vietinghoff, R. Förster, D. Hilfiker-Kleiner, H. Haller, T.V. Petrova, F.P. Limbourg, Loss of vascular endothelial notch signaling promotes spontaneous formation of tertiary lymphoid structures, Nat. Commun. 13 (2022) 2022.
[115] A.P. Risselada, M.F. Looije, A.A. Kruize, J.W. Bijlsma, J.A. van Roon, The role of ectopic germinal centers in the immunopathology of primary Sjogren's syndrome: a systematic review, Semin. Arthritis Rheum. 42 (2013) 368–376.
[116] R. Belfort Jr., N.F. Mendes, Identification of T and B lymphocytes in the human conjunctiva and lacrimal gland in ocular diseases, Br. J. Ophthalmol. 64 (1980) 217–219.
[117] M.K. Gatumu, K. Skarstein, A. Papandile, J.L. Browning, R.A. Fava, A.I. Bolstad, Blockade of lymphotoxin-beta receptor signaling reduces aspects of Sjögren's syndrome in salivary glands of non-obese diabetic mice, Arthritis Res. & Therap. 11 (2009) R24.
[118] R.A. Fava, S.M. Kennedy, S.G. Wood, A.I. Bolstad, J. Bienkowska, A. Papandile, J. A. Kelly, C.P. Mavragani, M. Gatumu, K. Skarstein, J.L. Browning, Lymphotoxin-beta receptor blockade reduces CXCL13 in lacrimal glands and improves corneal integrity in the NOD model of Sjögren's syndrome, Arthritis Res. & Therap. 13 (2011) R182.
[119] L. Shen, L. Suresh, J. Wu, J. Xuan, H. Li, C. Zhang, O. Pankewycz, J.L. Ambrus Jr., A role for lymphotoxin in primary Sjogren's disease, J. Immunol. 185 (2010) 6355–6363.
[120] S. Haskett, J. Ding, W. Zhang, A. Thai, P. Cullen, S. Xu, B. Petersen, G. Kuznetsov, L. Jandreski, S. Hamann, T.L. Reynolds, N. Allaire, T.S. Zheng, M. Mingueneau, Identification of novel CD4+ T cell subsets in the target tissue of Sjogren's syndrome and their differential regulation by the Lymphotoxin/LIGHT signaling Axis, J. Immunol. 197 (2016) 3806–3819.
[121] C.P. Robinson, S. Yamachika, D.I. Bounous, J. Brayer, R. Jonsson, R. Holmdahl, A. B. Peck, M.G. Humphreys-Beher, A novel NOD-derived murine model of primary Sjogren's syndrome, Arthritis Rheum. 41 (1998) 150–156.
[122] J. Kiripolsky, L. Shen, Y. Liang, A. Li, L. Suresh, Y. Lian, Q.Z. Li, D.P. Gaile, J. M. Kramer, Systemic manifestations of primary Sjögren's syndrome in the NOD. B10Sn-H2(b)/J mouse model, Clin. Immunol. 183 (2017) 225–232.
[123] J. Gao, S. Killedar, J.G. Cornelius, C. Nguyen, S. Cha, A.B. Peck, Sjogren's syndrome in the NOD mouse model is an interleukin-4 time-dependent, antibody isotype-specific autoimmune disease, J. Autoimmun. 26 (2006) 90–103.
[124] K. Tsubota, K.P. Xu, T. Fujihara, S. Katagiri, T. Takeuchi, Decreased reflex tearing is associated with lymphocytic infiltration in lacrimal glands, J. Rheumatol. 23 (1996) 313–320.